

# Characterization and Source Tracing of Nitrogenates and Halogens in Polyolefin Waste Pyrolysis Oils by Ultrahigh-Resolution FT-ICR MS

Gilles Dossche, Yannick Ureel, Martha L. Aguilera, Marvin Kusenberg, Ryan P. Rodgers, Maarten K. Sabbe, and Kevin M. Van Geem\*



Cite This: *Energy Fuels* 2025, 39, 22780–22796



[Read Online](#)

## ACCESS |

Metrics & More

## Article Recommendations

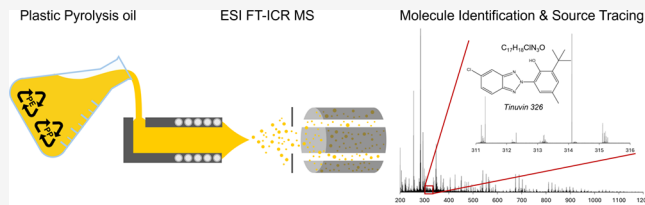
## SI Supporting Information

**ABSTRACT:** As the global tide of plastic waste surges, the need for scalable, effective recycling technologies has never been more urgent. Among emerging strategies, chemical recycling, particularly thermal pyrolysis, stands out as a promising approach for converting complex plastic waste streams, such as polyolefins, into valuable petrochemical feedstocks. However, the use of these pyrolysis oils is currently hampered by the presence of heteroatomic and halogen-containing species, which promote corrosion, fouling, coking and catalyst deactivation in downstream equipment. Detailed knowledge of those contaminants is required to design efficient purification techniques. Therefore, in this study, we employed ultrahigh-resolution 21 T Fourier transform ion cyclotron resonance mass spectrometry to determine the molecular composition of nitrogenates, nitrogen oxides, and halogens across a diverse set of pyrolysis oils. These pyrolysis oils originate from virgin and waste polyethylene, waste polypropylene, and waste mixed polyolefins. Combining positive and negative electrospray ionization facilitated the selective ionization of basic and acidic species, respectively. The remarkable similarities between virgin and waste pyrolysis oils revealed that a substantial fraction of the heteroatomic compounds originates from additives and/or processing agents. In addition to specific contaminants, pyrolysis oils also contain an abundance of aromatic compounds, which act as important “scavengers” of nitrogen and oxygen atoms. Among the halogens, chlorine dominated, with only traces of fluorine and no bromine. Chlorine was primarily present in specific additives and their corresponding breakdown products. Secondary reactions between chlorinated compounds and the hydrocarbon matrix appeared to be less important during thermal pyrolysis. Moreover, no dioxins were detected in any of the pyrolysis oils. The extraordinary level of detail in the results provides new fundamental insights into the formation, persistence, and possible origin of heteroatomic species in plastic waste pyrolysis oils, offering a molecular foundation for additive redesign, improved decontamination strategies and a cleaner path forward for chemical recycling.

## 1 INTRODUCTION

Starting from the discovery of Bakelite by Leo Baekeland in 1907,<sup>1</sup> plastics have emerged as one of the most widely used materials. Today, more than 460 million tonnes (Mt) of plastics are produced annually.<sup>2</sup> Due to their large-scale production and relatively short lifespan, more than 350 Mt of plastics reach end-of-life every year.<sup>2</sup> Only 9% is adequately recycled, with the remainder either incinerated (19%), landfilled (50%), or improperly disposed of (22%).<sup>2</sup> These figures highlight the urgent need for large-scale recycling technologies.

In general, plastic recycling can be classified into three categories: mechanical, physical, and chemical recycling.<sup>3</sup> In the case of mechanical recycling, plastic waste is first sorted, washed, shredded, and finally compounded into new materials.<sup>4</sup> Despite being the most commonly applied method today, mechanical recycling faces significant limitations, including polymer degradation, immiscibility in polymer blends, and impurity buildup across multiple cycles.<sup>5,6</sup>



To overcome these constraints, physical recycling has emerged as an alternative approach, in which polymers are extracted through selective dissolution and precipitation. The relatively low process temperatures reduce the risk of thermal degradation and allow for partial impurity removal.<sup>7</sup> However, suitable environmentally friendly solvents are not always available.<sup>8</sup> As such, chemical recycling, i.e., the breakdown of waste plastics into monomers or petrochemical feedstocks, is expected to become the most important plastic recycling technology.<sup>3</sup>

Among chemical recycling methods, pyrolysis is the most widely applied, mainly due to the ability to process heterogeneous and contaminated plastic waste streams.<sup>9</sup>

Received: August 11, 2025

Received: August 11, 2025

Accepted: November 14, 2025

Published: November 20, 2025



During pyrolysis, plastics undergo thermochemical decomposition under an inert gas atmosphere, yielding a complex mixture commonly referred to as pyrolysis oil.<sup>10–12</sup> Driven by free radical chemistry, this process generates a broad product distribution that includes all major PIONA (Paraffins, Iso-paraffins, Olefins, Naphthenes and Aromatics) classes, spanning a wide carbon number range.<sup>13</sup>

Despite the differences in product yields, both thermal and catalytic pyrolysis oils contain a broad range of contaminants, including heteroatoms such as nitrogen, oxygen, sulfur, chlorine, and trace metals.<sup>13,14</sup> These contaminants originate from either polymer additives, organic and inorganic residues that accumulate during use, or traces of ill-sorted polymers. Their presence lowers the quality of the pyrolysis oils and necessitates additional pretreatment steps before use as petrochemical feedstocks.<sup>15</sup> The most abundant contaminants in plastic waste pyrolysis oils are heteroatomic species containing oxygen, nitrogen, and halogens, such as chlorine.<sup>13,14,16</sup> These heteroatomic species hamper the use of pyrolysis oils as they are known to cause corrosion, increased fouling and coking in steam cracking, and potential poisoning of downstream catalysts.<sup>13,17</sup> Additionally, nitrogen-containing species may promote the formation of explosive gums during steam cracking.<sup>18</sup> Considering the associated safety hazards and the detrimental effect on the on-stream time, it is essential to minimize these contaminants as much as possible.

The concentration of contaminants can be reduced with additional treatments, both before and after pyrolysis. Prior to pyrolysis, plastic waste is sorted and washed. Foreign materials, such as metals, glass, paper, and organic residues, can be removed from waste streams using sieves, air classifiers, magnetic attraction, induced magnetic repulsion, and sink float separation, among other methods.<sup>19</sup> Heavier plastics, such as polyvinyl chloride (PVC), polycarbonate (PC), and acrylonitrile butadiene styrene polymer (ABS), can be separated from a polyolefin waste stream based on their density differences.<sup>20,21</sup> Removing these materials is critical for lowering the heteroatom load, particularly chlorine, nitrogen, and oxygen, in the resulting pyrolysis oils.

More advanced techniques, such as near or short-wave infrared spectroscopy, hyperspectral imaging spectroscopy and laser-induced breakdown spectroscopy, enable further polymer separation.<sup>22</sup> However, despite the advances in sorting technology, it is still impossible to obtain monostreams from heterogeneous plastic waste streams.<sup>19</sup> These limitations highlight the importance of chemical recycling approaches, such as pyrolysis, which are uniquely suited to handle complex, mixed plastic waste streams. To meet industrial feedstock specifications for contaminant levels, several upgrading technologies already exist, e.g., hydrotreating, depth filtration, distillation, and dehalogenation.<sup>21,23–26</sup> Optimizing these existing methods and developing new ones requires detailed chemical analyses to uncover the molecular composition of contaminants in plastic waste pyrolysis oils.

Numerous analytical techniques have been used to characterize plastic pyrolysis oils. Historically, the focus was on the characterization of the hydrocarbon fraction. Comprehensive two-dimensional gas chromatography (GC × GC) coupled with flame ionization detection (FID) and mass spectrometry (MS) has been widely applied for the characterization of the hydrocarbon fraction of a wide variety of plastic pyrolysis oils.<sup>13,27–29</sup> Additionally, GC × GC coupled to a nitrogen chemiluminescence detector (NCD) has been used

for the analysis of the nitrogenates in mixed plastic waste pyrolysis oils. For example, Toraman et al.<sup>14</sup> reported the detection of 1 wt % of nitrogen (elemental analysis), with the majority of nitrogenates identified as nitriles, along with smaller fractions of pyridines, quinolines, and indoles. A similar study by Kusenberg et al.<sup>13</sup> characterized three different plastic waste pyrolysis oils. Based on the GC × GC-NCD results, the nitrogen content (elemental) ranged from 0.0029 to 0.1144 wt % of nitrogen, depending on the feedstock. In this case, anilines were the most important type of nitrogenates, followed by quinolines, amines, pyridines, and pyrroles. Halogens were measured by combustion ion chromatography (CIC), revealing chlorine levels between 137 and 474 ppmw of chlorine, which is substantially above the three ppmw maximum tolerated in industrial steam cracker feedstocks.<sup>15</sup> Only traces of bromine and no fluorine were detected in any of the pyrolysis oils.

However, GC × GC is generally less effective for high-molecular-weight, heteroatom-rich compounds due to their low volatility and thermal instability.<sup>30</sup> While combustion elemental analysis, inductively coupled plasma optical emission spectroscopy (ICP-OES), or combustion ion chromatography (CIC) can quantify specific heteroatoms, these techniques cannot determine the molecular formulas of impurities. Fourier transform ion cyclotron resonance mass spectrometry (FT-ICR MS) is a complementary technique capable of identifying high-molecular-weight species potentially containing multiple heteroatoms.<sup>31–39</sup>

For instance, Mase et al.<sup>31</sup> analyzed nitrogenates and nitrogen oxides in a mixed plastic pyrolysis oil. The detected molecules were categorized into heteroatom classes based on the number of nitrogen and oxygen atoms, i.e.,  $N_xO_y$ , where  $x$  and  $y$  indicate the number of nitrogen and oxygen atoms in the molecular formula, respectively. While these class labels emphasize the heteroatom content, all identified species also contain carbon and hydrogen. The predominant nitrogenate classes were N1 and N2, with pyridine, quinoline, carbazole, and indole moieties identified as the most common structural motifs. Among nitrogen oxides, N1O1, N1O2, N2O1, and N2O2 were the most abundant classes. Furthermore, the type of oxygen functionality was found to be class-dependent: N1O1 and N2O1 species were primarily associated with alcohol groups, while N1O2 and N2O2 species contained predominantly carboxyl functionalities. However, these findings were based on a single plastic pyrolysis oil, and specific contaminant sources were not identified. The influence of additives, contaminants, and traces of nonpolyolefin polymers on pyrolysis oil composition, as well as how these interactions vary across different types of polymers, remains an active area of investigation.

In this work, we employed ultrahigh-resolution 21 T FT-ICR MS to investigate the molecular composition of nitrogenates, nitrogen oxides, and halogen-containing species in four different plastic pyrolysis oils: virgin low-density polyethylene (LDPE), postconsumer polyethylene (PE), postconsumer polypropylene (PP), and postconsumer mixed polyolefins (MPO) pyrolysis oil. All samples were analyzed using both positive and negative electrospray ionization [(+)-ESI and (-)-ESI], which selectively ionize basic and acidic compounds, respectively.<sup>40</sup> This combination of dual ionization modes and exceptional resolving power of 21 T FT-ICR MS enabled the detailed identification of high-molecular-weight heteroatomic species across diverse plastic waste

streams. Beyond molecular characterization, the results also provide critical insight into the origin and persistence of these contaminants, revealing key links to common plastic additives and processing agents.

## 2. MATERIALS AND METHODOLOGY

**2.1. Materials.** Polyolefinic plastic pyrolysis oils from four different sources, i.e., one virgin low-density polyethylene (LDPE) pyrolysis oil and three postconsumer plastic waste pyrolysis oils, polyethylene (PE), polypropylene (PP), and mixed polyolefins (MPO) pyrolysis oil, were analyzed in this work. The virgin LDPE pyrolysis oil and the three postconsumer plastic pyrolysis oils were produced in earlier work performed by Abbas-Abadi et al.<sup>41</sup> and Kusenberg et al.,<sup>13</sup> respectively. The virgin LDPE was a film-grade LDPE LD 150 series sample from ExxonMobil with a density of 923 kg m<sup>-3</sup> (ASTM D1505) and a melt flow index of 0.75 g/10 min (at 190 °C/2.16 kg, ASTM D1238). The postconsumer PE originates from a sorted PE film fraction. Both sorted postconsumer PP and MPO stem from rigid applications. An indicative composition of these three waste streams was provided by Kusenberg et al.<sup>13</sup> and is given in Table 1.

**Table 1. Indicative Composition of the Original Waste PE, Waste PP, and Waste MPO Fraction<sup>a</sup>**

	waste PE fraction	waste PP fraction	waste MPO fraction
PE (wt %)	97	12	53
PP (wt %)	1	88	46
others (wt %)	~2	<0.1	~1

<sup>a</sup>Others include polyethylene terephthalate, ethylene vinyl alcohol, polyamide, polyvinyl(idene) chloride, polyurethane, and ethylene vinyl acetate. Data taken from ref 13.

These three postconsumer plastic waste fractions, provided by the Belgian recycling company Ecco, are representative outlet streams for a typical European plastic waste sorting facility. Trace amounts of (in)organic residues and other polymers are present in these waste streams due to imperfect sorting and cleaning.

All four plastic pyrolysis oils were produced using a continuously operated pilot-scale pyrolysis unit, consisting of a single-screw extruder directly coupled to a heated, continuously stirred tank reactor (CSTR). A constant feeding rate of 1 kg h<sup>-1</sup> was used to introduce the plastic waste samples into the reactor, which was operated at 450 °C and atmospheric pressure. To evacuate any remaining air, prior to the experiments, the reactor was flushed for several minutes with N<sub>2</sub>. Oil samples were collected once steady-state conditions were achieved. For more details about the experimental setup, the reader is referred to the work of Kusenberg et al.<sup>13</sup>

The elemental composition of the three postconsumer plastic waste streams and the corresponding pyrolysis oils were characterized by combustion elemental analysis, GC × GC-NCD, and combustion ion chromatography (CIC) in previous work performed by Kusenberg et al.<sup>13</sup> The results are presented in Table 2. Due to the absence of contaminants accrued during usage and the limited presence of additives, no supplementary analysis was performed for the virgin sample.

**2.2. 21 T FT-ICR MS.** A custom-built 21 T FT-ICR mass spectrometer, equipped with both (+)ESI and (-)ESI, was used for the analysis of respectively basic and acidic nitrogen-, nitrogen oxide-, and halogen-containing species present in the four pyrolysis oils.<sup>42,43</sup> In both cases, the plastic pyrolysis oils were dissolved in a 1:1 (volumetric ratio) toluene:methanol solution at a concentration of 50 µg mL<sup>-1</sup>. The use of methanol was necessary to fully dissolve polar compounds, including those derived from plastic additives and other contaminants present in the plastic pyrolysis oils. Subsequently, the samples were infused at a rate of 0.55 µL min<sup>-1</sup> and ionized with a needle voltage of 3.6 kV and -3.2 kV for (+)ESI and (-)ESI,

**Table 2. Elemental Composition of the Postconsumer Plastic Waste and the Corresponding Pyrolysis Oils<sup>a</sup>**

	waste PE fraction		waste PP fraction		waste MPO fraction	
	solid waste	pyrolysis oil	solid waste	pyrolysis oil	solid waste	pyrolysis oil
C [wt %]	84.3	85.3	85.5	86.3	85.3	86.2
H [wt %]	13.9	14.5	14.1	13.7	14.2	13.7
N [wt %]	0.2	0.004	<0.1	0.0029	0.2	0.1143
O [wt %]	1.6	0.2	0.3	<0.1	0.3	<0.1
S [wt %]	<0.1	0.0009	<0.1	0.0005	<0.1	0.0046
Cl [ppmw]	2100	143	1400	137	3600	474
F [ppmw]	<40	<LOD	<40	<LOD	<40	<LOD
Br [ppmw]	<50	22	<50	<LOD	<50	<LOD

<sup>a</sup>Data taken from ref 13.

respectively. The produced ions were analyzed with a custom-built 21 T FT-ICR mass spectrometer.<sup>42</sup> An external multipole ion trap equipped with automatic gain control was used for the accumulation of  $2 \times 10^6$  charges within approximately 1–5 ms.<sup>44</sup> To improve signal-to-noise in the mass range of interest, ion depletion was applied to suppress highly abundant background ions with *m/z* values between 306 and 334. This method selectively removes dominant gas-phase contaminants, thereby enhancing the detection of sample-derived peaks.<sup>45</sup> Following ion accumulation and transfer to the ICR cell, ions were excited to an *m/z*-dependent radius to optimize dynamic range and maximize peak detection. The dynamically harmonized ICR cell operated at a trapping potential of 6 V. For all samples, 100 time-domain transients of 3.2 s each were acquired and averaged using Predator software. A methanol blank sample was used to verify that the FT-ICR MS instrument was cleaned, prior to the analysis. Internal calibration was performed using an extended homologous alkylation series of high-abundance peaks. Peaks were detected above a  $6\sigma$  baseline root-mean-square (RMS) noise threshold, followed by automated elemental composition assignment. To ensure full spectral coverage, calibration included paraffins, olefins, and diolefins, representing double bond equivalent (DBE) values of zero, one, and two, respectively. Molecular formula assignments and data visualization in DBE versus carbon number plots were carried out using PetroOrg software. The DBE, defined in eq 1 with C, H, X, and N, the number of carbon, hydrogen, halogen, and nitrogen atoms, respectively, is a measure of the number of double bonds and cyclic rings present in a hydrocarbon and thus reflects the degree of unsaturation. As shown in the formula, the DBE depends on the valence of the constituting atoms: -0.5 for monovalent atoms (H, X), 0 for divalent atoms (O), +0.5 for trivalent atoms (N), and +1.0 for tetravalent atoms (C). As such, the DBE is independent of oxygen content.

$$\text{DBE} = C - \frac{H}{2} - \frac{X}{2} + \frac{N}{2} + 1 \quad (1)$$

For data analysis, only molecular formulas with a mass error below ~0.10 ppm and compound classes with a relative abundance of at least 0.10% in one of the four pyrolysis oil samples were retained for data interpretation. Size-scattered DBE versus carbon number plots were used to visualize and interpret the data. In these plots, the area of each data point is proportional to the relative abundance of the corresponding molecular formula. The relative abundance of a specific molecular class, e.g., all species containing carbon, hydrogen, and only one nitrogen atom, i.e., the N1 class, was determined by summing the abundances of all molecular formulas in that class and normalizing this sum to the total signal of all detected formulas. This normalization was performed separately for each ionization mode. Note that, if detected, the <sup>13</sup>C-topologues were included in the analysis and their relative abundance was added to the relative abundance of the corresponding class. Separate size-scattered DBE

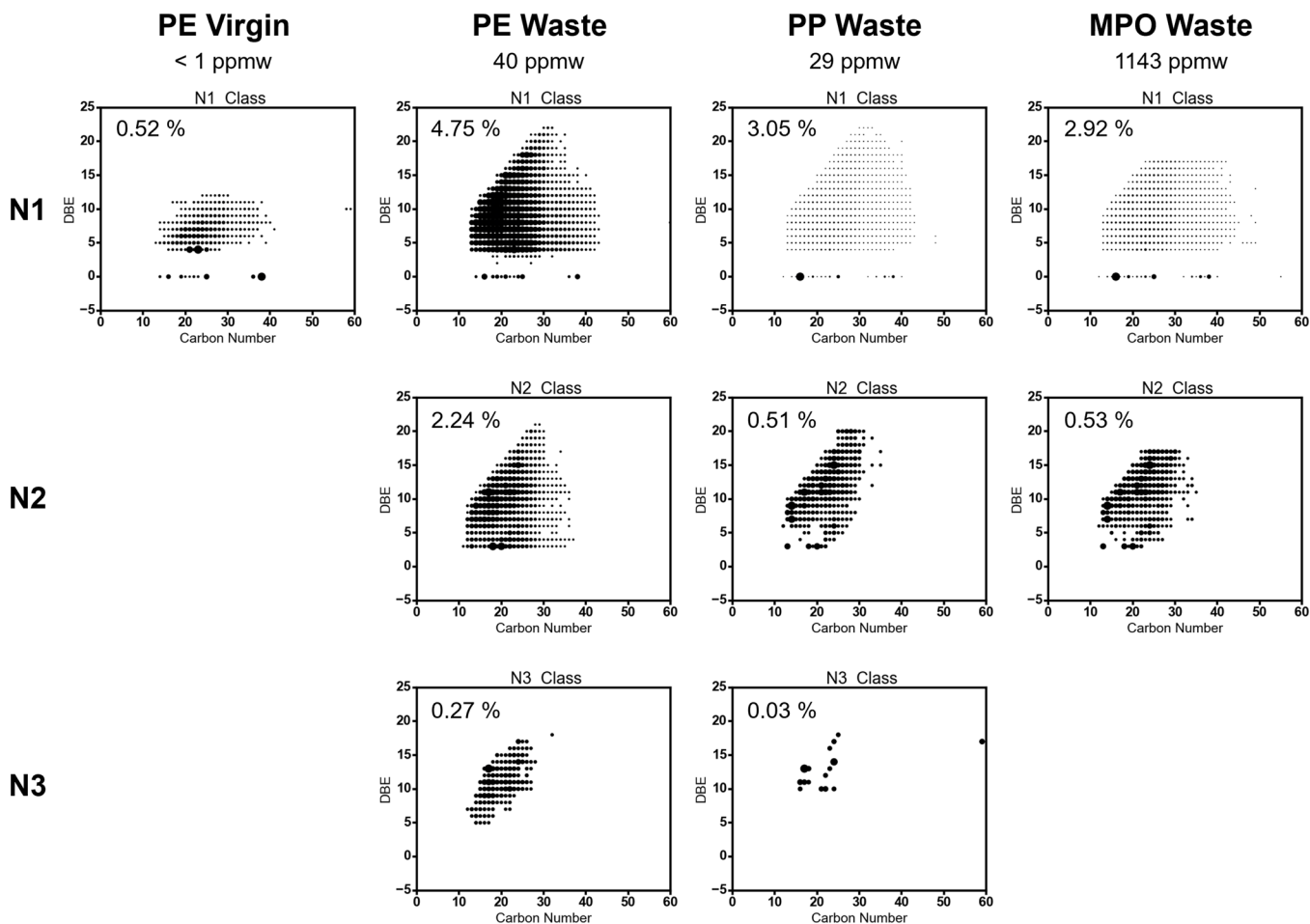


**Figure 1.** DBE versus carbon number plots derived from (+)ESI 21 T FT-ICR MS for nitrogenates in virgin LDPE, waste PE, waste PP, and waste MPO pyrolysis oil. The area of the dots is proportional to the relative abundance of the respective molecular formula. The total amount of nitrogen in the pyrolysis oils reported by Kusenberg et al.<sup>13</sup> is given at the top of each column in ppmw and the relative abundance per molecular class for this ionization mode is given in the graphs.

versus carbon number plots for the detected <sup>13</sup>C-topologues can be found in the Supporting Information (Figures S8–S16).

### 3. RESULTS AND DISCUSSION

Oxygen, nitrogen, and halogens are among the most abundant heteroatoms in plastic waste pyrolysis oils.<sup>13,14,16</sup> Given their negative impact on processing and compliance with industrial feedstock specifications, understanding their molecular composition, structure, and origin is essential. The following sections detail the analysis of nitrogenates, nitrogen oxides, and halogen-containing species in the four pyrolysis oils. The analysis of the pure hydrocarbons are given in Figure S1 of the Supporting Information. Results on oxygen-containing species have been previously reported by Ureel et al.<sup>39</sup>

**3.1. Nitrogen.** The elemental nitrogen content in plastic waste pyrolysis oils typically ranges in the low thousands of ppmw of nitrogen, substantially exceeding the 100 ppmw industrial petrochemical feedstock limit for naphtha and approaching the 2000 ppmw threshold for gas oil-type feedstocks.<sup>15</sup> Three different sources of nitrogen can be distinguished: polymer additives such as colorants, antistatics, lubricants, etc.; nitrogen-containing polymers such as polyamides (PA) and polyurethanes (PUR); and nitrogen-containing contaminants such as food residues, i.e., amino acids, and nitrogen-containing detergents.<sup>15,46</sup> Depending on

the nitrogen source, different decomposition pathways prevail, e.g., amino acids can decompose into ammonia,<sup>47</sup> while PUR and PA yield large fractions of (aromatic) nitrogenates such as nitriles and amines, which may further decompose into ammonia and hydrogen cyanide.<sup>48–50</sup>

**3.1.1. (+)ESI.** Basic nitrogen compounds, such as amines, pyridines, and quinolines, are efficiently ionized by positive-mode electrospray ionization [(+)ESI].<sup>31</sup> The results of (+)ESI FT-ICR MS, along with the elemental composition of the four pyrolysis oils reported by Kusenberg et al.<sup>13</sup> are shown in Figure 1. The elemental composition of the three postconsumer plastic waste streams and their corresponding pyrolysis oils is summarized in Table 2.

Although the nitrogen content in the polyethylene (PE) and mixed polyolefin (MPO) waste streams is comparable, i.e., approximately 2000 ppmw of nitrogen, the resulting pyrolysis oils show a marked difference: 40 ppmw of nitrogen in PE pyrolysis oil versus 1143 ppmw of nitrogen in MPO pyrolysis oil. The nitrogen concentration in the polypropylene (PP) pyrolysis oil is also similar to that of the PE pyrolysis oil, despite the initially lower concentration in the PP waste, i.e., less than 1000 ppmw of nitrogen.

Because of the absence of nitrogen-containing additives and contaminants, the nitrogen content of the virgin low-density polyethylene (LDPE) pyrolysis oil is assumed to be negligible.

Note that the FT-ICR MS results are only semiquantitative. Because ionization efficiency varies with chemical functionality and ionization mode, certain compounds may appear disproportionately abundant in the spectra. Quantitative comparisons of relative abundances are therefore only valid for compounds with similar chemical functionality within the same sample. These limitations help explain discrepancies between the elemental composition reported by Kusenberg et al.<sup>13</sup> and the relative abundances derived from FT-ICR MS.

In the virgin LDPE pyrolysis oil, only N1 compounds were detected. In contrast, the postconsumer PE and PP pyrolysis oils contained N1, N2, and N3 nitrogenates, while the MPO pyrolysis oil showed the presence of N1 and N2 nitrogenates only. No N4 compounds were detected in any of the plastic pyrolysis oils by (+)ESI. For these postconsumer waste pyrolysis oils, the abundance of nitrogenates decreased sharply with increasing nitrogen atom count per molecule. This trend contrasts with the oxygenate analysis performed by Ureel et al.<sup>39</sup> in which the relative abundance only significantly decreases beyond the O2 class. In the virgin LDPE pyrolysis oil, the N1 species consisted of an abundant fraction of saturated aliphatic amines. These saturated aliphatic amines, which have a DBE of zero, likely originate from surfactants, corrosion inhibitors, antistatic agents, or other processing agents used in reactor cleaning or laboratory preparation.  $C_{38}H_{79}N$  is the most abundant nitrogenate with a DBE of zero in the virgin LDPE pyrolysis oil, followed by  $C_{25}H_{53}N$ ,  $C_{16}H_{35}N$ ,  $C_{36}H_{75}N$ , and  $C_{19}H_{41}N$ .  $C_{38}H_{79}N$  most likely originates from distearyl dimethyl ammonium chloride ( $C_{38}H_{80}ClN$ , Figure 2), a quaternary ammonium salt

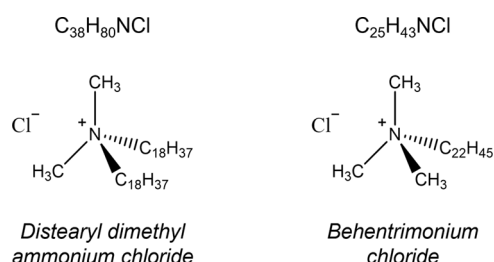


**Figure 2.** Molecular structures of distearyl dimethyl ammonium chloride and behentrimonium chloride (docosyltrimethylammonium chloride).

frequently used as fabric softener, antistatic agent, detergent, etc.<sup>51</sup> This hypothesis is further supported by the presence of known breakdown products such as  $C_{36}H_{75}N$ ,  $C_{20}H_{43}N$ , and  $C_{19}H_{41}N$ , that can be formed after loss of alkyl chain(s) from the nitrogen atom. Moreover, this salt is readily ionized and therefore efficiently detected by FT-ICR MS. Similarly,  $C_{25}H_{53}N$  is likely derived from behentrimonium chloride (docosyltrimethylammonium chloride,  $C_{25}H_{54}ClN$ ; Figure 2), a commonly used antistatic agent.<sup>46</sup> Again, possible breakdown products, such as  $C_{23}H_{49}N$  and  $C_{22}H_{47}N$ , have been detected. The detection of both the original additives and their corresponding breakdown products indicates that these additives were not fully decomposed under the aforementioned pyrolysis conditions. According to the pyrolysis experiments performed by Pappijn et al.,<sup>52</sup> diethylamine decomposition only starts around 500 °C. Despite the longer residence times and the significantly larger saturated aliphatic amines in the present work, at 450 °C, it is expected that saturated aliphatic amines will not fully decompose.

Another potential source of nitrogenates in virgin LDPE is the polymerization initiator, e.g., azobisisobutyronitrile (AIBN). AIBN decomposes into  $N_2$  and two 2-cyanoprop-2-yl radicals. However, both species are too low in mass to be detected under the current FT-ICR MS conditions. In addition to the detected aliphatic amines, a substantial fraction of (poly)aromatic nitrogenates was also observed in the virgin LDPE pyrolysis oil, including aromatic amines, anilines, pyridines, and quinolines. Overall,  $C_{23}H_{41}N$ , a nitrogenate with a DBE of four, has the highest abundance. These nitrogenates with a DBE of four could be species with a pyridine group, species formed via the reaction of a benzyl radical and a saturated aliphatic amine, a reaction between ammonia and the hydrocarbon matrix, etc. In general, species with a DBE value of at least four are expected to be (poly)aromatics. Based on their uniform and broad distribution, combined with the fact that these types of heteroatomic (poly)aromatic species were detected in the majority of the molecular classes of all samples indicates that they are mainly formed during secondary reactions. For the remainder of this manuscript, we will use the term aromatics for both mono- and polyaromatics. A similar distribution of N1 species is observed across all three postconsumer plastic pyrolysis oils. As in the virgin LDPE pyrolysis oil, a distinct series of species with a DBE of zero and carbon numbers between 12 and 55 is present, along with a broad variety of aromatic nitrogenates. However, opposed to virgin LDPE pyrolysis oil,  $C_{16}H_{35}N$  is the most abundant nitrogenate with a DBE of zero in all postconsumer waste pyrolysis oils. Moreover, postconsumer plastic waste pyrolysis oil exhibits a broader range of aromatic nitrogenates. This is expected to be due to the additional presence of contaminants and heteroatomic polymers, like PUR, PA and PET. These impurities, which are not found in virgin plastics, can decompose during pyrolysis, thereby releasing nitrogenates, and heteroatomic species in general, which could participate in secondary reactions.<sup>48,53</sup>

The GC × GC-NCD analysis performed by Kusenberg et al.<sup>13</sup> indicates that anilines are the dominant type of nitrogenates in all three postconsumer plastic waste pyrolysis oils. The higher share of aromatic nitrogenates compared to aliphatic nitrogenates is expected to be due to the higher stability of the former. This is perfectly illustrated by the comparison of the C–N bond dissociation energies of diethylamine and aniline, reported in Figure 3. The aromatic

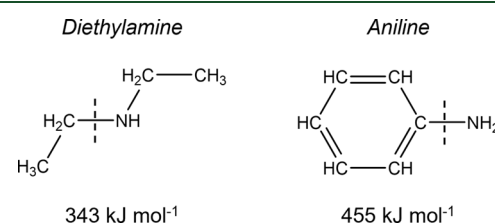


**Figure 3.** Bond dissociation energies for the C–N bond in diethylamine and aniline. Data obtained from refs 54, 55.

C–N bond in aniline is approximately 112 kJ mol<sup>-1</sup> stronger than the aliphatic C–N bond in diethylamine. Consequently, aliphatic amines will decompose more easily compared to anilines. As a result, addition reactions between ammonia and aromatic hydrocarbons will result in a more favorable (lower) reaction enthalpy and yield more stable anilines, compared to the aliphatic amines. Similar trends have been reported by

Ureel et al.<sup>39</sup> for C–O bonds, although the energy difference is smaller, at 83 kJ mol<sup>−1</sup>.

The tendency of ammonia to react preferentially with aromatic hydrocarbons, combined with the higher stability of the resulting nitrogenates, may also explain the substantially higher concentration of nitrogen in waste MPO pyrolysis oil (1143 ppmw) compared to waste PE pyrolysis oil (40 ppmw), despite similar nitrogen levels in the original plastic waste. Considering that a substantial fraction of nitrogenates present in plastic waste is converted into ammonia, and that MPO pyrolysis oil contains a higher share of aromatic hydrocarbons than PE pyrolysis oil, i.e., 13.6 wt % versus 3.9 wt %,<sup>13</sup> MPO pyrolysis oil offers more aromatic species for addition reactions with ammonia. As a result, nitrogen is more readily incorporated into stable nitrogenates in the hydrocarbon matrix, leading to a higher nitrogen content in MPO pyrolysis oil. Alternatively, there could be a difference in the chemical structure of the nitrogenates initially present in the PE and MPO plastic waste. However, since both feeds are post-consumer chemical waste, a similar chemical profile can be expected. This conclusion is further supported by the high degree of similarity in the (+)ESI FT-ICR MS results, depicted in Figure 1. Note that the relative abundances derived from (+)ESI FT-ICR MS show an opposite trend, i.e., the relative abundance of the N1 class in waste PE pyrolysis oil is higher than the relative abundance of the N1 class in waste MPO pyrolysis oil. This difference is an artifact of the aforementioned semiquantitative nature and normalization.

In addition to anilines and amines, MPO pyrolysis oil also contains a substantial fraction of quinolines and pyridines, as detected by GC × GC-NCD.<sup>13</sup> Quinolines are structures often present in polymer dyes, such as pinacyanol or sodium 2-(1,3-dioxoindan-2-yl)quinolinedisulfonate, also known as quinoline yellow WS.<sup>56</sup> Pyridinic structures are present in various food additives, e.g., nicotinic acid, 2-acetylpyridine, etc., and cosmetic products such as hair and skin products, e.g., nicotinamide, zinc pyrithione, etc.

N1 nitrogenates with a DBE of one, two, or three, corresponding to nitriles, nitrogenated naphthalenes, or nitrogenated (di)olefins, have not been detected in either virgin LDPE, PP, or MPO pyrolysis oil. In PE pyrolysis oil, a small fraction of N1 nitrogenates with a DBE of two and three was detected. The absence of such species with a DBE of one, two, or three in most samples suggests that these types of species are not present in the original solid waste fractions and are not significantly formed during pyrolysis. This is likely due to the lower bond dissociation energies of C–N and N–H bonds compared to C–C and C–H bonds, combined with the substantial weakening of C–C and C–H bonds in the vicinity of nitrogen atoms (see Figure 4). These effects favor the fragmentation of amines with a DBE of zero into lower-molecular-weight nitrogen compounds, rather than the formation of larger N1 species with a DBE equal to one, two or three.<sup>57</sup> Moreover, due to the high stability of aromatic nitrogenates (see Figure 3) it is energetically unfavorable to reduce the DBE below a value of four. In addition, the high abundance of pure hydrocarbons with a DBE of two and three, previously reported by Ureel et al.,<sup>39</sup> indicates that the formation of the corresponding nitrogenates via secondary reactions is less important. Toraman et al.<sup>14</sup> detected 5 wt % of nitriles in mixed plastic waste pyrolysis oil; however, these nitriles were primarily (alkylated)benzonitriles. These aromatic

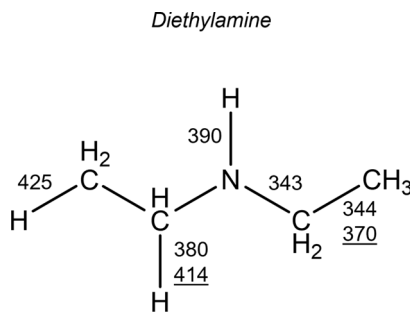


**Figure 4.** Bond dissociation energies for diethylamine (solid) and the alkane analogue (underlined). Data obtained from ref 55.

nitriles have a DBE of at least six, which is consistent with the results obtained in the present work.

N2 and N3 compounds were not detected in virgin LDPE pyrolysis oil. This is expected to be due to the lack of N2 and N3 compounds in the original virgin LDPE, the absence of N2 and N3 contaminants, and the low likelihood of their formation via secondary reactions between either ammonia and N1 nitrogenated compounds or N1 nitrogenated compounds mutually. The latter is based on the fact that the concentration of hydrocarbons is several orders of magnitude higher than that of nitrogenates.

In contrast, for the plastic waste pyrolysis oils, the composition of N2 nitrogenates in PE pyrolysis oil differs slightly from that observed in PP and MPO pyrolysis oil. Despite the broad distribution of N2 nitrogenates observed in the PE pyrolysis oil, three compounds are particularly abundant, i.e.,  $\text{C}_{17}\text{H}_{16}\text{N}_2$ ,  $\text{C}_{18}\text{H}_{34}\text{N}_2$ , and  $\text{C}_{20}\text{H}_{38}\text{N}_2$ , with a DBE of eleven, three, and three, respectively. The first compound is likely a degradation product of quinoline dyes used for polymer coloration, while the latter two could correspond to imidazole or imidazoline structures stemming from, e.g., food and cosmetic residues. These three nitrogenates are also present in PP and MPO pyrolysis oils, albeit at a lower abundance. In those samples, the dominant N2 species are  $\text{C}_{14}\text{H}_{14}\text{N}_2$  and  $\text{C}_{24}\text{H}_{22}\text{N}_2$ . 1,2-di-p-tolyldiazene ( $\text{C}_{14}\text{H}_{14}\text{N}_2$ ) and 1-(4-methylnaphthalen-1-yl)-2-(2,3,6-trimethylnaphthalen-1-yl)diazene ( $\text{C}_{24}\text{H}_{22}\text{N}_2$ ), depicted in Figure 5, are likely sources for these N2 nitrogenates. Both diazenes are degradation products of so-called azo dyes, which are commonly applied for coloring textiles, cosmetics, and food. The degradation temperature of these azo dyes spans a wide range from 250 °C up to temperatures above 600 °C,<sup>58,59</sup> depending on the nature and position of the substituents. Upon thermal decomposition, the C–N bond breaks, yielding both an aromatic and an azo radical. The latter may further decompose, releasing molecular nitrogen ( $\text{N}_2$ ) and an additional aromatic radical.<sup>59</sup>

N3 nitrogenates are considerably less abundant than N1 and N2 species but display a similar composition in both PE and PP postconsumer plastic pyrolysis oils. In both cases,  $\text{C}_{17}\text{H}_{13}\text{N}_3$ , with a DBE of 13, is the most abundant compound. A potential structure for this component is depicted in Figure 5. The benzotriazole functionality, commonly found in UV stabilizers such as 2-(Benzotriazol-2-yl)-4,6-bis(2-methylbutan-2-yl)phenol ( $\text{C}_{22}\text{H}_{29}\text{N}_3\text{O}$ ), is a likely source.<sup>60</sup> These stabilizers are routinely added to plastics to prevent UV-induced degradation, including cracking and discoloration. This hypothesis is further supported by the detection of

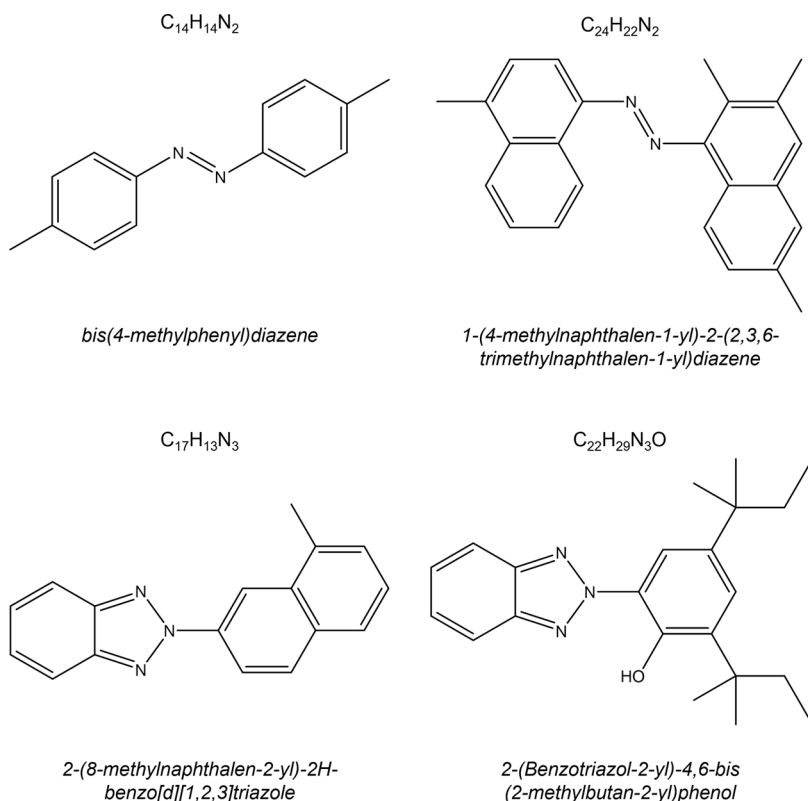


**Figure 5.** Molecular structures of bis(4-methylphenyl)diazene and 1-(4-methylnaphthalen-1-yl)-2-(2,3,6-trimethylnaphthalen-1-yl)diazene, top, and 2-(8-methylnaphthalen-2-yl)-2H-benzo[d][1,2,3]triazole and 2-(benzotriazol-2-yl)-4,6-bis(2-methylbutan-2-yl)phenol, bottom.

$C_{22}H_{29}N_3O$  as one of the most abundant  $N3O$  species in the (+)ESI spectra (see Figure S2).

3.1.2.  $(-)$ ESI. Acidic nitrogenates, such as pyrroles, imidazoles, etc., are primarily detected by  $(-)$ ESI.<sup>40</sup> The  $(-)$ ESI FT-ICR MS results for the four pyrolysis oils are shown in Figure 6. Based on the GC  $\times$  GC-NCD analysis of the plastic waste pyrolysis oils conducted by Kusenberg et al.,<sup>13</sup> pyrroles represent only a minor fraction of the detected nitrogenates. In general, pyrrolic structures are uncommon in plastic additives. However, they can be formed via the decomposition of benzotriazoles into indoles and nitriles or carbazoles. For example, the pyrolysis of 1-arylbenzotriazoles, also known as the Graebe-Ullman synthesis, results in the formation of more stable carbazoles.<sup>61</sup> In contrast, vinyl-benzotriazoles decompose into N-phenylketenimines, which are further converted into nitriles, and indoles at elevated temperatures.<sup>62</sup> Both carbazoles and indoles contain pyrrolic functionalities and can thus be detected by  $(-)$ ESI.

The virgin LDPE and the waste PP pyrolysis oil have a comparable N1 nitrogenate composition, with abundant species clustered around DBEs of nine, ten, and eleven. The N1 species with a DBE of nine are most likely carbazole derivatives, while those with a DBE of ten and eleven may correspond to carbazoles with unsaturated side chains or more general (fused) aromatic nitrogenates. In contrast, the waste PE and MPO pyrolysis oils reveal a much broader distribution of N1 nitrogenates, with  $C_{21}H_{17}N$  as the most abundant composition. Additionally, the high relative abundance of N1 nitrogenates with a DBE of twelve is characteristic of benzocarbazoles. Note that N2 and N3 nitrogenates were only detected in the waste PE and MPO pyrolysis oil. Again, a high level of similarity is found between both pyrolysis oils. For

N2 nitrogenates, two major peaks can be identified,  $C_{20}H_{38}N_2$  and  $C_{18}H_{34}N_2$ . These two compounds were also observed in the (+)ESI spectra, suggesting the presence of both acidic and basic functionalities. These two compositions are also visible in the DBE versus carbon number plots reported by Mase et al.,<sup>31</sup> albeit at a lower relative abundance. Similar to (+)ESI data,  $C_{17}H_{13}N_3$  is the most abundant N3 nitrogenate in both oils. A small fraction of highly aromatic N4 nitrogenates was detected exclusively in the waste MPO pyrolysis oil, and is likely due to its higher aromatic content compared to the waste PE and PP pyrolysis oils.

**3.2. Nitrogen Oxides.** Analogous to nitrogenates, nitrogen oxides present in plastic waste typically originate from either plastic additives, nitrogen oxide-containing polymers or contaminants. However, compared to nitrogenates, nitrogen oxides are less likely to be formed via secondary reactions during pyrolysis, as the released ammonia and carbon monoxide are more likely to react with pure hydrocarbons rather than with the small fraction of oxygenated or nitrogenated hydrocarbons, respectively. Likewise, nitrogenates and oxygenates are more likely to react with pure hydrocarbons rather than mutually.

3.2.1. (+)ESI. The relative abundance of the various nitrogen oxides detected by (+)ESI FT-ICR MS is depicted in Figure 7. In all four pyrolysis oils, N1O1 nitrogen oxides have the highest relative abundance, with a general decline in relative abundance as the number of nitrogen and oxygen atoms increases. The reason for this trend is likely 2-fold. First, plastic additives and organic residues typically contain only a limited number of nitrogen and oxygen atoms. Second, ammonia and carbon monoxide released during pyrolysis are more likely to react with pure hydrocarbons rather than with nitrogenates,

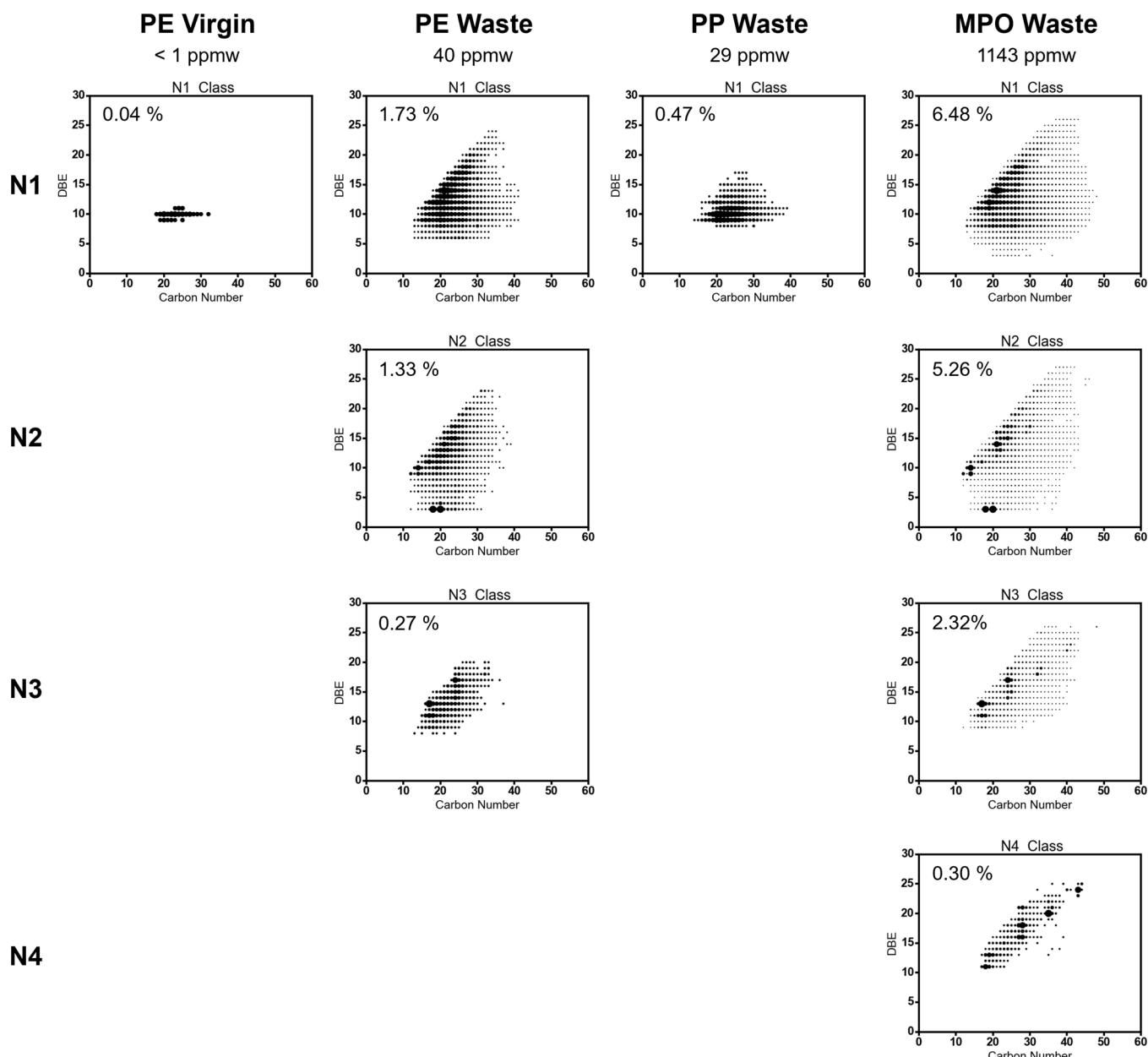


**Figure 6.** DBE versus carbon number plots derived from (−)ESI 21 T FT-ICR MS for nitrogenates in virgin LDPE, waste PE, waste PP, and waste MPO pyrolysis oil. The area of the dots is proportional to the relative abundance of the respective molecular formula. The total amount of nitrogen in the pyrolysis oils reported by Kusenberg et al.<sup>13</sup> is given at the top of each column in ppmw and the relative abundance per molecular class for this ionization mode is given in the graphs.

oxygenates, or nitrogen oxides. As a result, the formation of nitrogen oxides via secondary reactions becomes less probable, the higher the number of nitrogen and/or oxygen atoms already present in the compound. Note that this trend is less pronounced in the case of virgin LDPE pyrolysis oil, which could be due to the overall low abundance of nitrogen oxides in virgin LDPE pyrolysis oil. Interestingly, in waste PP and MPO pyrolysis oil, N<sub>2</sub>O<sub>2</sub> nitrogen oxides are more abundant than N<sub>2</sub>O<sub>1</sub> nitrogen oxides. This anomaly is attributed due to the presence of specific compounds, as discussed in the coming paragraphs.

In all four pyrolysis oils, C<sub>22</sub>H<sub>43</sub>NO, with a DBE of two, is the most abundant N1O1 molecular formula. This formula is consistent with erucamide (docos-13-enamide), a common fatty acid primary amide used in plastics. C<sub>18</sub>H<sub>35</sub>NO and

C<sub>20</sub>H<sub>39</sub>NO, which were also detected with a relatively high abundance, may correspond to oleamide and eicosenamide, respectively. Erucamide and fatty acid primary amides in general are widely used processing aids that act as slip agents and internal processing lubricants for polyolefins and are hence detected in all samples.<sup>46,63,64</sup> A study performed by Jug et al.<sup>65</sup> has found that oleamide could leach from (plastic) labware into analytical samples. However, considering the broad range of fatty acid primary amides detected in the four plastic pyrolysis oils and the slower migration of erucamide compared to oleamide,<sup>66</sup> it is expected that a substantial fraction of the overall relative abundance originates from the pyrolysis oil samples, rather than from labware contamination. This is further supported by the fact that the use of these additives is not limited to plastic labware and considering that complete

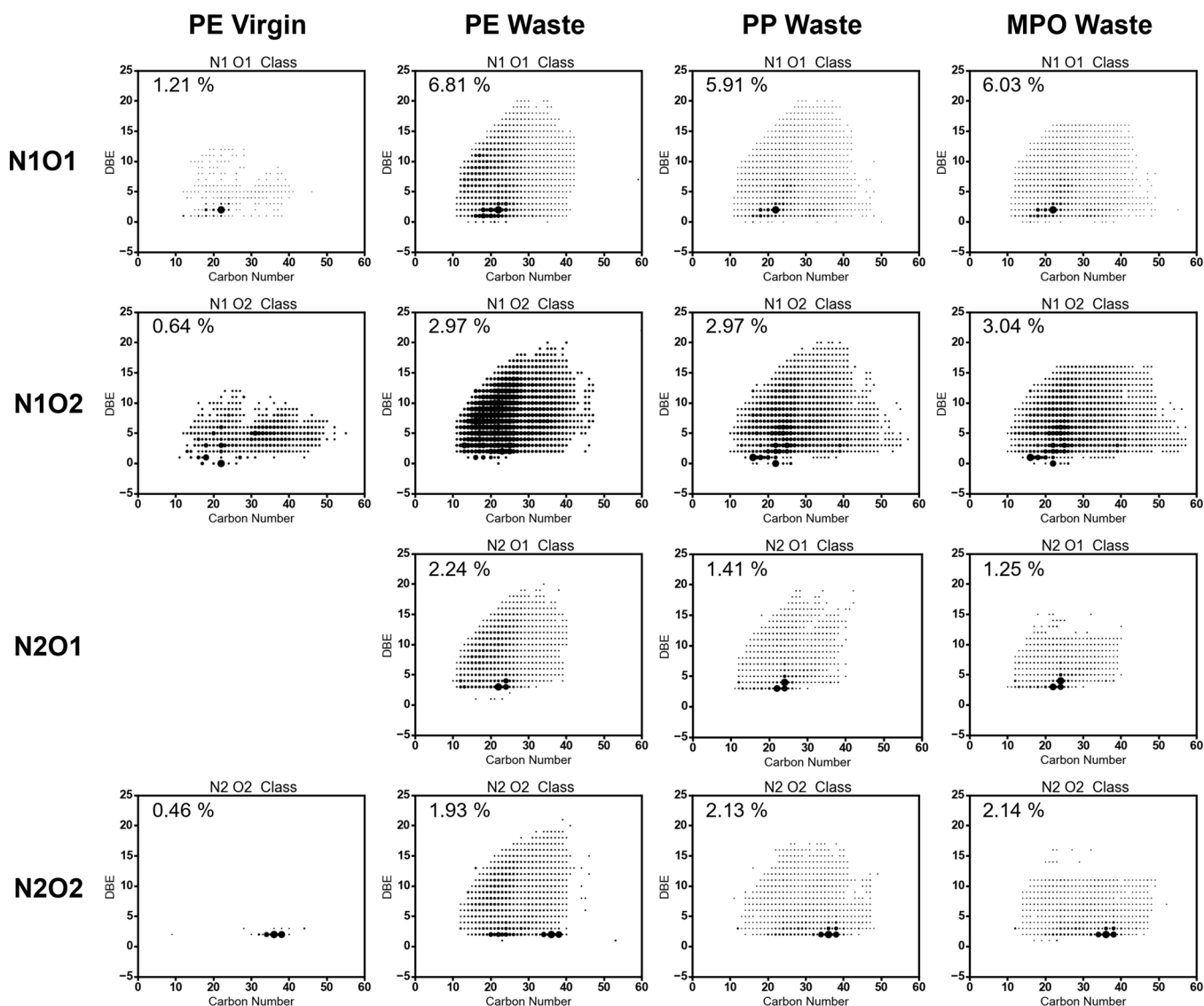


**Figure 7.** DBE versus carbon number plots derived from (+)ESI 21 T FT-ICR MS for nitrogen oxides in virgin LDPE, waste PE, waste PP, and waste MPO pyrolysis oil. The area of the dots is proportional to the relative abundance of the respective molecular formula. The relative abundance per molecular class for this ionization mode is given in the graphs.

decomposition of fatty acid primary amides during pyrolysis is rather unlikely. Next to these specific fatty acid primary amides, and consistent with the results obtained for nitrogenates, there is wide variety of species, especially those consistent with aromatic compounds. This is more pronounced for postconsumer plastic waste pyrolysis oils.

A broad range of N1O2 nitrogen oxides has been detected across all four pyrolysis oils. Two major peaks can be distinguished in the virgin LDPE pyrolysis oil,  $C_{22}H_{47}NO_2$  and  $C_{18}H_{37}NO_2$ .  $C_{22}H_{47}NO_2$ , which has a DBE of zero, is consistent with stearyl diethanolamine. Stearyl diethanolamine and alkyl ethanolamines in general are frequently used as antistatic agents.<sup>67</sup> On the other hand,  $C_{18}H_{37}NO_2$  may correspond to either palmitoylethanolamide or sphingosine. The aforementioned peaks are also prominent in waste PP and MPO pyrolysis oils. However, for both oils,  $C_{16}H_{33}NO_2$  had the highest abundance and is consistent with lauryl betaine. These alkyl betaines, such as lauryl betaine ( $C_{16}H_{33}NO_2$ ) and oleyl betaine ( $C_{22}H_{43}NO_2$ ), are widely used in personal care products, which could still be present in traces in

postconsumer waste.<sup>68</sup> The same N1O2 formulas were also detected in the PE pyrolysis oil, albeit at a lower relative abundance. In this case, instead of specific dominant peaks, there is a region of higher abundance which is located at carbon numbers below 25 and DBE values in the range of zero to fifteen. Considering the absence of specific dominant peaks, this region is expected to mainly consist of secondary reaction products. The reduced abundance beyond this region, i.e., at higher carbon numbers and/or higher DBE values, is consistent with the hydrocarbon distribution reported by Kusenberg et al.<sup>13</sup> This high-abundant region is also visible in waste PP and waste MPO pyrolysis oil. However, due to the presence of specific dominant peaks, this is less pronounced.

N2O1 nitrogen oxides were detected exclusively in the plastic waste pyrolysis oils. Three major molecular formulas can be distinguished,  $C_{22}H_{42}N_2O$ ,  $C_{24}H_{46}N_2O$ , and  $C_{24}H_{44}N_2O$ .  $C_{22}H_{42}N_2O$  is expected to be oleyl hydroxyethyl imidazoline, see Figure 8. These imidazoline derivatives are frequently used as corrosion inhibitors, rheology modifiers, emulsifiers, antistatic agents, adhesion promoters in paints and

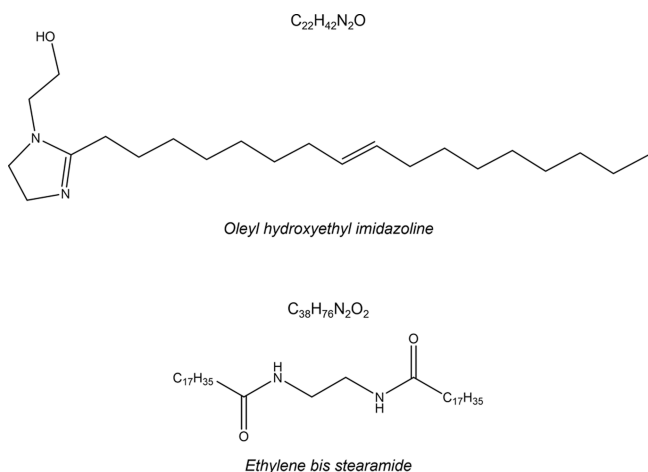


**Figure 8.** Molecular structure of oleyl hydroxyethyl imidazoline, top, and ethylene bis stearamide (EBS), bottom.

inks, etc.<sup>69,70</sup> Upon pyrolysis,  $C_{22}H_{42}N_2O$  may decompose to  $C_{20}H_{38}N_2$ , a species also observed with relatively high abundance in both (+)ESI and (−)ESI spectra.  $C_{24}H_{46}N_2O$  is expected to have a similar structure, e.g., 2-[2-(8-Heptadecen-1-yl)-4,4-dimethyl-4,5-dihydro-1H-imidazol-1-yl]-ethanol or 4-[2-(1-Heptadecen-1-yl)-4,5-dihydro-1H-imidazol-1-yl]-1-butanol, which may similarly decompose into  $C_{20}H_{38}N_2$  or  $C_{24}H_{44}N_2O$  through double bond formation.

Three major  $N_2O_2$  nitrogen oxide peaks were observed in all four pyrolysis oils, i.e.,  $C_{38}H_{76}N_2O_2$ ,  $C_{36}H_{72}N_2O_2$ , and  $C_{34}H_{68}N_2O_2$ . All three species have a DBE of two and are thus most likely diamide structures. For instance,  $C_{38}H_{76}N_2O_2$  matches the molecular formula of ethylene bis stearamide (EBS), see Figure 8, which is widely used as slip agent for polyolefin film production, internal processing lubricant to enhance flow and mold release, filler dispersant, etc.<sup>63,64,71</sup> The other two species,  $C_{36}H_{72}N_2O_2$  and  $C_{34}H_{68}N_2O_2$ , are presumed to share similar diamide backbones. This hypothesis is further supported by the fact that these diamides are

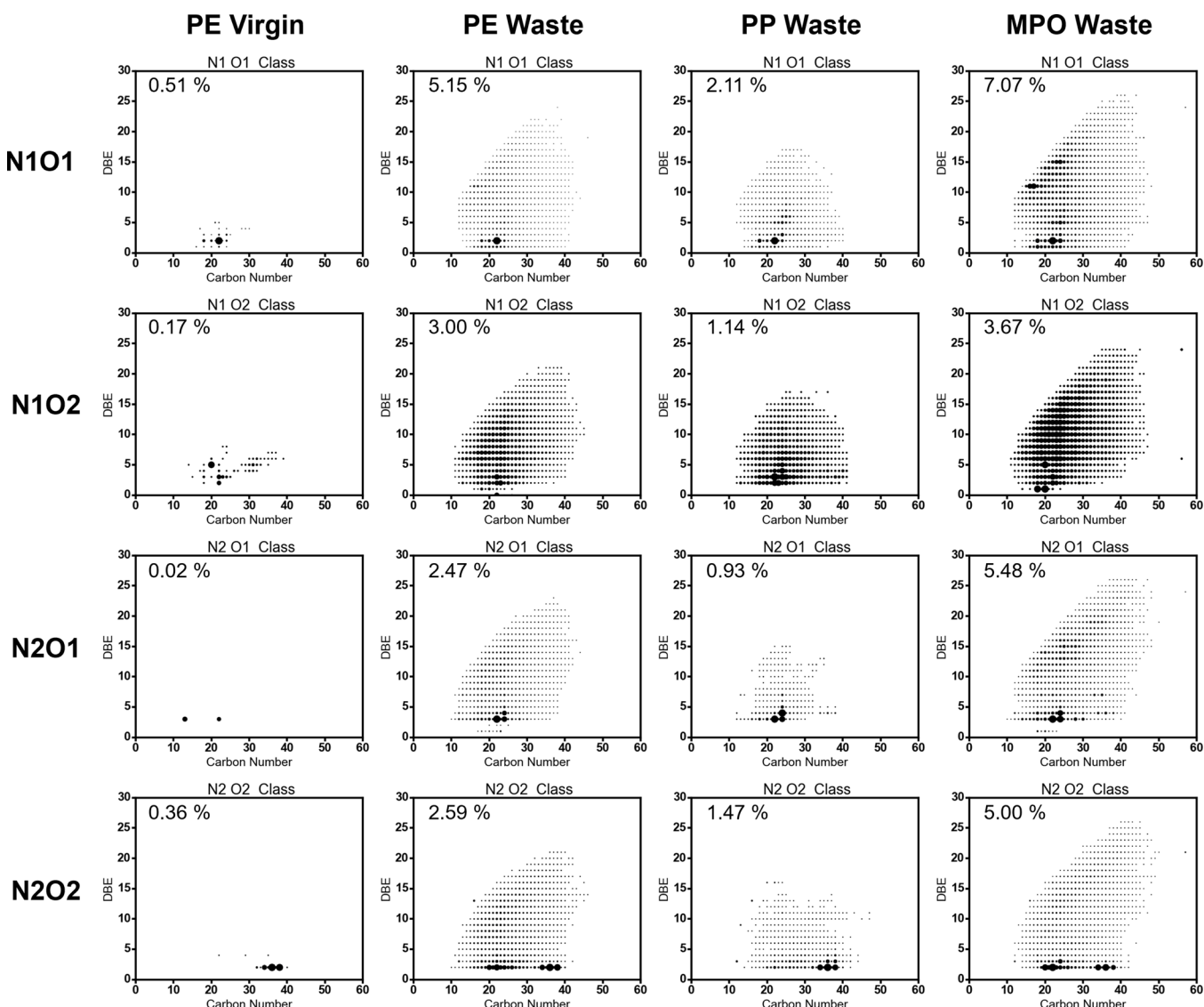


**Figure 9.** DBE versus carbon number plots derived from (−)ESI 21 T FT-ICR MS for nitrogen oxides in virgin LDPE, waste PE, waste PP, and waste MPO pyrolysis oil. The area of the dots is proportional to the relative abundance of the respective molecular formula. The relative abundance per molecular class for this ionization mode is given in the graphs.

produced starting from diamines and fatty acids that typically span a distribution of alkyl chain lengths.<sup>71</sup>

**3.2.2. (−)ESI.** The (−)ESI FT-ICR MS results for nitrogen oxides are depicted in Figure 9. As in the (+)ESI data,  $C_{22}H_{43}NO$ , expected to be erucamide based on its molecular formula, is the most abundant N1O1 species in all four pyrolysis oils. The overall N1O1 profiles are comparable between the two ionization modes, except for the waste MPO pyrolysis oil, which displays additional abundant species, i.e.,  $C_{16}H_{13}NO$ ,  $C_{17}H_{15}NO$ ,  $C_{23}H_{19}NO$ , and  $C_{24}H_{21}NO$ , not observed in (+)ESI. Compared to (+)ESI, only a limited number of N1O2 compounds have been detected in virgin LDPE pyrolysis oil.  $C_{20}H_{33}NO_2$  is the most abundant N1O2 composition and could be myristyl nicotinate. Waste PE pyrolysis oil displays a broader N1O2 profile, consistent with the (+)ESI data, but without any dominant peaks.  $C_{22}H_{41}NO_2$  is the most abundant N1O2 nitrogen oxide in waste PP pyrolysis oil. This could be an unsaturated breakdown product of stearyldiethanolamine ( $C_{22}H_{47}NO_2$ ), which also appears in high abundance in the (+)ESI spectra.

Three major N1O2 peaks were detected in waste MPO pyrolysis oil, i.e.,  $C_{20}H_{41}NO_2$ ,  $C_{18}H_{37}NO_2$ , and  $C_{20}H_{33}NO_2$ .  $C_{20}H_{41}NO_2$  is expected to be stearoylethanolamide, whereas  $C_{18}H_{37}NO_2$ , also prominent in the (+)ESI spectra, may be palmitoylethanolamide or sphingosine. N-acylethanolamines, such as stearoylethanolamide and palmitoylethanolamide, are fatty acid derivatives commonly used in detergents, corrosion inhibitors, cosmetics, and are also found in trace amounts in biological systems.<sup>72</sup> Sphingosine, by contrast, is present in sphingolipids, an important type of membrane lipids.<sup>73</sup>

Consistent with the (+)ESI results,  $C_{22}H_{42}N_2O$ ,  $C_{24}H_{46}N_2O$ , and  $C_{24}H_{44}N_2O$  are the most abundant N2O1 nitrogen oxides in waste plastic pyrolysis oils. Two N2O1 nitrogen oxide species have been identified in the virgin LDPE pyrolysis oil, i.e.,  $C_{13}H_{24}N_2O$  and  $C_{22}H_{42}N_2O$ . Finally, the same three N2O2 nitrogen oxides also dominate the (−)ESI spectra. Additionally, waste PE and MPO pyrolysis oil contain an abundant series of smaller N2O2 species with a DBE of two and carbon numbers between 20 and 26. These are expected to be breakdown products of  $C_{38}H_{76}N_2O_2$ ,  $C_{36}H_{72}N_2O_2$ , and  $C_{34}H_{68}N_2O_2$ .

Overall, the specific dominant molecular formulas of nitrogenates and nitrogen oxides detected in this work were not abundantly present in the mixed plastic pyrolysis oil analyzed by Mase et al.<sup>31</sup> This discrepancy may stem from differences in plastic waste feedstock or pyrolysis process conditions, including a lower pyrolysis temperature of 410 °C in their study compared to 450 °C in the present work. Secondary reaction products, generally present in lower abundance and less dependent on the type of impurities, are in greater agreement.

Despite the relatively low abundance of nitrogenates and nitrogen oxides in virgin plastic pyrolysis oil, overall, their molecular composition closely matches that of postconsumer plastic waste pyrolysis oils. This similarity indicates that a substantial portion of the nitrogen-containing compounds originates from additives and contaminants introduced during processing, rather than from use-related exposure. The same observation was made for the oxygenates in previous work performed by Ureel et al.<sup>39</sup>

Considering the strict industrial feedstock specifications regarding nitrogen and oxygen content, it is thus crucial to limit the use of heteroatom-containing compounds. One

solution is to develop polymer additives and processing agents that support recyclability. In the absence of suitable alternatives, these heteroatomic additives and contaminants could be removed from the plastic waste stream prior to the pyrolysis process. Several additive extraction methods exist, such as batch single- and multistage extraction, ultrasonic treatment, microwave assisted methods, supercritical fluid extraction, accelerated solvent extraction and dissolution–precipitation. However, further research and optimization remain necessary.<sup>46</sup> As such, the polymer additives and processing agents identified in this work provide valuable insight into the major impurities present in typical plastic waste streams and represent a solid foundation for advancing targeted extraction strategies. Next to additives and processing agents, it is evident that heteroatom-rich polymers should be removed from the plastic waste stream prior to the pyrolysis process. These heteroatom-rich polymers generally have a higher density than polyolefins and can be separated from a plastic waste stream using flotation techniques.<sup>5</sup>

Apart from these specific compounds, a significant fraction of highly unsaturated nitrogenates and nitrogen oxides was observed, likely reflecting the higher stability of aromatic structure. These species, which can be formed via the decomposition of contaminants or via secondary reactions between heteroatomic species and the hydrocarbon matrix, act as effective “scavengers” of heteroatoms, such as nitrogen and oxygen. This relationship between the aromatic content and the nitrogen content in the pyrolysis oils is clearly illustrated by the comparison of the waste PE and the waste MPO pyrolysis oil. Because of their high stability, a posteriori removal of these species in pyrolysis oils is rather difficult. Therefore, polymer additives and processing agents containing aromatically bonded nitrogen and/or oxygen should thus be avoided as much as possible or removed prior to pyrolysis, e.g., using the aforementioned extraction techniques. Moreover, polymers producing a large amount of aromatics during pyrolysis, such as polystyrene (PS)<sup>74</sup> and polyethylene terephthalate (PET),<sup>75</sup> should be removed from the polyolefin waste stream as much as possible prior to the pyrolysis process. As already mentioned, most heteroatom-rich polymers, like PET, and in extension also higher density polymers, such as PS, can be effectively separated from polyolefins using flotation techniques.<sup>5</sup> Nevertheless, complete removal is rarely achieved, and a residual fraction of nitrogenates and nitrogen oxides will persist in postconsumer plastic waste pyrolysis oils. If the nitrogen concentration exceeds the feedstock limitations for industrial stream crackers, the pyrolysis oil can be diluted with fossil naphtha or subjected to additional pretreatments steps.<sup>15</sup> Hydrotreating, more specific catalytic hydrodenitrogenation, is currently the most mature and widely used technology for the removal of nitrogen from oils.<sup>76</sup> Alternative approaches include liquid–liquid extraction, adsorption, complexation with metallic salts, etc.<sup>76</sup> Further development and optimization of these nitrogen removal technologies, e.g., selection of adequate solvents, adsorbents, etc., can be guided by the detailed molecular characterization of nitrogenates and nitrogen oxides in the plastic pyrolysis oils as presented in this work.

**3.3. Halogens.** Halogen-containing species pose a significant challenge in the chemical recycling of plastic waste. During pyrolysis, halogens can be released as highly corrosive gases such as hydrogen fluoride (HF), hydrogen chloride (HCl) and hydrogen bromide (HBr).<sup>77</sup> Because of their corrosive nature, they can damage processing equipment

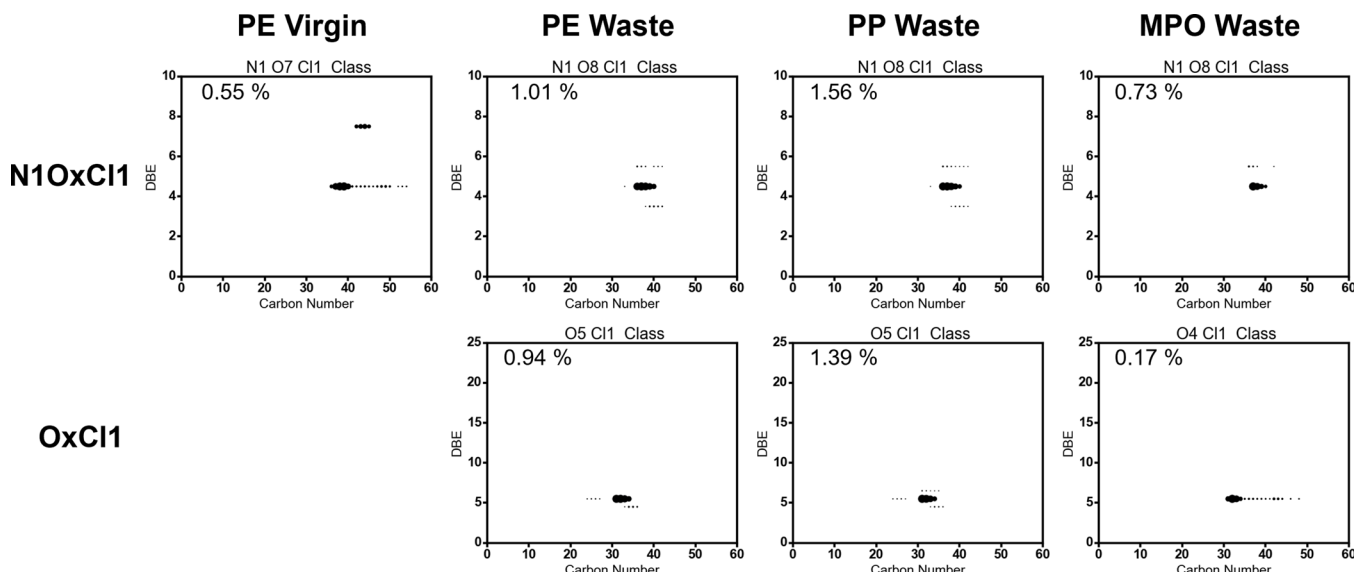


**Figure 10.** DBE versus carbon number plots derived from (−)ESI 21 T FT-ICR MS for the most abundant chlorine nitrogen oxides (top) and chlorine oxides (bottom) classes in virgin LDPE, waste PE, waste PP, and waste MPO pyrolysis oil. The area of the dots is proportional to the relative abundance of the respective molecular formula. The relative abundance per molecular class for this ionization mode is given in the graphs.

and disrupt continuous operation. Additionally, these gases also contribute to the deactivation of downstream catalysts.<sup>77</sup>

Halogens are introduced into plastic waste through various sources. Common polymer additives, such as brominated and chlorinated flame retardants, are well-known contributors.<sup>78</sup> In addition, the presence of halogen-rich polymers, such as polyvinyl chloride (PVC) and polyvinylidene chloride (PVDC), originating, from e.g., multilayer packaging or ill-sorted mixed plastic waste streams, also contributes to the occurrence of chlorine.<sup>5,79</sup> Residual chlorine may also derive from Ziegler–Natta catalysts used in polyolefin production,<sup>80</sup> as well as from exposure to halide-containing salts during use or disposal, particularly in postconsumer waste streams.<sup>77</sup>

The halogen content of the three postconsumer plastic waste streams and their corresponding pyrolysis oils was quantified by Kusenberg et al.<sup>13</sup> using combustion ion chromatography (CIC). The data is summarized in Table 2. Chlorine emerged as the predominant halogen in both the solid plastic wastes and the corresponding pyrolysis oils. No significant amount of bromine or fluorine was detected in any of the postconsumer plastic waste pyrolysis oils by CIC. To effectively reduce halogen levels in pyrolysis oils, identifying their main sources and understanding their thermal decomposition behavior remains critical.

**3.3.1. (−)ESI.** (−)ESI FT-ICR MS allows the detection of halogenated organic molecules. Fluorine and chlorine were the only halogens that were detected. Fluorine was detected only in the waste PE and waste PP pyrolysis oils. In waste PE pyrolysis oil, only the F1 class was observed. These F1 species, with a DBE between 29 and 33 and a carbon number in the range of 39 to 67, represent highly aromatic species with a single fluorine atom (see Figure S3). For waste PP pyrolysis oil, O8S1F1 was the only fluorine-containing class. These O8S1F1 species have a DBE in the range of one to three and carbon numbers in the range of 25 to 44 (see Figure S3). These types of large organic species with a high number of heteroatoms, especially oxygen atoms, generally indicate a biological source, e.g., species containing glucose-derived groups. The most likely source of large oxygen-rich species

with one sulfur atom are sulfolipids. These sulfolipids are present in cell membranes of plants and cyanobacteria.<sup>81</sup> The fluor atom is expected to originate from a secondary reaction with a fluor-containing compound.

Chlorine has been detected in all four pyrolysis oils. In virgin LDPE pyrolysis oil, N1O7Cl1 was the only chlorinated class that has been detected. In contrast, the chlorinated species identified in the plastic waste pyrolysis oils were more diverse and predominantly belonged to chlorine nitrogen oxide classes ( $N_xO_yCl_1$ ) and chlorine oxide classes ( $O_xCl_1$ ). Relatively small fractions of chlorine sulfides ( $S1Cl_1$ ) and chlorine sulfur oxides ( $O_xS1Cl_1$ ) were also detected. Isoabundance DBE versus carbon number plots for the most abundant chlorine nitrogen oxide and chlorine oxide classes are summarized in Figure 10. The complete set of chlorine-containing classes is provided in the Supporting Information, see Figures S4–S7.

The N1O7Cl1 class was identified in both virgin LDPE and waste MPO pyrolysis oil. The most dominant compounds in this class are  $C_{37}H_{67}ClNO_7$ ,  $C_{38}H_{69}ClNO_7$  and  $C_{39}H_{71}ClNO_7$ , all with a DBE of 4.5.  $C_{36–40}H_{65–73}ClNO_x$  in general, are among the most abundant chlorine nitrogen oxides detected across the plastic pyrolysis oils (see Figure 10). The consistent DBE versus carbon number patterns observed for chlorine nitrogen oxides across the four plastic pyrolysis oils, shown in Figure 10 and in greater detail in Figure S4, suggest a common origin. Based on the assigned molecular formulas, these species are likely glycolipids, such as cerebroside, which have been chlorinated. These glycolipids are biological species that naturally occur in biological cell membranes.<sup>82</sup> Their presence in the pyrolysis oils likely stems from residual biological contamination in postconsumer plastic waste, such as food residues or cosmetics. While these compounds may originate as glycolipids, modifications during pyrolysis, such as dehydration, fragmentation, recombination, etc., could change their DBE values or alter their structure. Alternatively, detected DBE values around four could indicate the presence of aromatic moieties, either introduced from contaminants (e.g., surfactants, dyes) or formed in situ. How these high-mass, heteroatom-containing species survive pyrolysis remains an

open question. Their persistence suggests that they are either inherently thermally stable or formed as secondary products later in the pyrolysis process, when localized temperatures or reactive environments may favor stabilization through aromatization or radical recombination. The presence of chlorine may be attributed to the formation of chlorine adducts during the (−)ESI-process.<sup>40</sup> It is currently not clear how these biological contaminants can end up in virgin LDPE pyrolysis oil. However, no other potential sources could be identified. For Cl1O4, Cl1O5 and Cl1O<sub>x</sub> in general, a similar pattern is found in the plastic waste pyrolysis oils with a peak around C<sub>31–34</sub>H<sub>52–58</sub>ClO<sub>x</sub>, see Figures 10 and S5 in more detail. These species likely share a common precursor, possibly altered during pyrolysis or ionization.

In addition to the previously discussed species, waste PP pyrolysis oil also contains a substantial fraction of species belonging to the Cl1N3O1 class (see Figure S4). This class almost exclusively consists of C<sub>17</sub>H<sub>18</sub>ClN<sub>3</sub>O, which is consistent with 2-(2-hydroxy-3-tert-butyl-5-methylphenyl)-5-chlorobenzotriazole, a frequently used antioxidant and UV stabilizer (see Figure 11).<sup>83</sup> For this species specifically, i.e., the

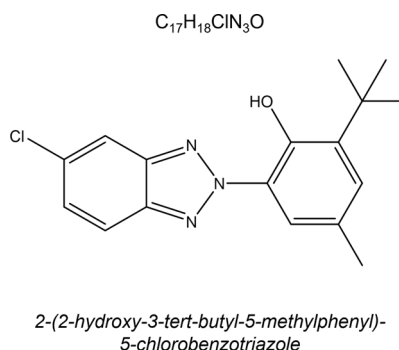


**Figure 11.** Molecular structure of 2-(2-hydroxy-3-tert-butyl-5-methylphenyl)-5-chlorobenzotriazole, also referred to as bumetizole or Tinuvin 326.

most abundant chlorinated compound, a <sup>37</sup>Cl-topologue has been detected. The relative abundance of the two topologues was found to be in agreement with the natural relative abundance of <sup>35</sup>Cl- and <sup>37</sup>Cl-isotopes.

Finally, despite recent concerns regarding the potential formation of polychlorinated dibenzo-p-dioxins (PCDDs) and polychlorinated dibenzofurans (PCDFs), collectively referred to as dioxins, during the pyrolysis of plastic waste,<sup>84–86</sup> no such species were detected in any of the plastic pyrolysis oils analyzed in this work. Indeed only chlorine oxides consisting of one chlorine atom were observed by (−)ESI FT-ICR MS. Paladino and Moranda,<sup>86</sup> for example, analyzed the flue gases of a catalytic plastic waste pyrolysis pilot plant and detected small concentrations of dioxins. However, compared to the feedstock used in the present work, their plastic waste stream contained 2–4 wt.% of PVC. The presence of a substantial fraction of PVC could be a potential source for dioxins.<sup>85</sup> The minimal amount of chlorine-containing species present in the plastic waste streams pyrolyzed in the present work, see Table 2, could be a reason for the absence of PCDDs and PCDFs. These findings demonstrate the importance of removing PVC and other chlorine-rich materials prior to pyrolysis. Additional research is needed to evaluate the potential for dioxin formation under conditions involving higher chlorine content or different feedstocks.

Overall, the detected chlorinated molecules mainly consisted of a limited set of contaminants breaking down, and few secondary reaction products were found. This suggests that HCl released during thermal pyrolysis does not significantly react with the hydrocarbon matrix under the tested conditions. Chlorinated additives were detected in all pyrolysis oils; however their use should be minimized as they release corrosive HCl, which hampers chemical recycling infrastructure. In the PP pyrolysis oil, one of the most abundant chlorine-containing molecular formulas (C<sub>17</sub>H<sub>18</sub>ClN<sub>3</sub>O) is consistent with 2-(2-hydroxy-3-tert-butyl-5-methylphenyl)-5-chlorobenzotriazole, a commonly used antioxidant and UV stabilizer. While the exact identity cannot be confirmed solely based on accurate mass, the detection highlights the contribution of chlorinated stabilizers to the halogen content. To ensure compatibility with circular economy goals, the development and adoption of “design-for-recycling” strategies, particularly those aimed at eliminating or replacing chlorinated compounds, will be essential for enabling efficient and scalable chemical recycling of plastic waste.

#### 4. CONCLUSIONS

Ultrahigh-resolution 21 T FT-ICR MS using both (+)ESI and (−)ESI has been used for the molecular characterization of nitrogenates, nitrogen oxides, and halogens in virgin LDPE, waste PE, waste PP, and waste MPO pyrolysis oil. The remarkable level of similarities between the heteroatomic compounds found in the virgin LDPE pyrolysis oil and those in the three postconsumer plastic waste pyrolysis oils indicates that a substantial fraction of these species originates from additives and/or processing agents. Considering the industrial specifications for petrochemical feedstocks, it is thus of utmost importance to limit their usage and to develop better alternatives.

For both nitrogenates and nitrogen oxides, the relative abundance of a molecular class was found to decrease with the number of heteroatoms. An exception is the N<sub>2</sub>O<sub>2</sub> nitrogen oxides in waste PP and MPO pyrolysis oil. This is due to the relatively high abundance of long-chain diamides originating from frequently used slip agents, internal processing lubricants, and related additives.

Apart from these specific contaminants, a significant fraction of highly unsaturated nitrogenates and nitrogen oxides was also observed. The majority of these species are expected to be aromatics, based on their DBE values and carbon number distributions. Because of their higher bond dissociation energies, aromatic nitrogenates are more stable than their aliphatic analogues. Moreover, this higher stability also favors the addition of ammonia, which is released from nitrogen-containing contaminants during pyrolysis, to aromatic hydrocarbons over aliphatic ones. Thus, aromatic hydrocarbons act as “scavengers” for nitrogen and oxygen atoms, contributing to the formation of relatively stable heteroatomic species. This difference in stability was reflected in the higher nitrogen content of MPO pyrolysis oil compared to PE pyrolysis oil and in the absence of N1 nitrogenates with a DBE of one, two, and three.

Chlorine and fluorine were the only halogens detected. Fluorine was only detected in waste PE and waste PP pyrolysis oil, primarily as high-DBE species with high carbon numbers. In contrast, chlorine was detected in all four pyrolysis oils. The corresponding molecular formulas are consistent with known additives, such as Tinuvin 326 in waste PP pyrolysis oil, as well

as their expected degradation products. Little secondary reaction products were detected, indicating that the HCl released during thermal pyrolysis does not significantly react with the hydrocarbon matrix. Despite recent concerns, no dioxins were detected in any of the pyrolysis oils.

Overall, the detected molecular formulas provide strong evidence for the presence of additive-derived and contaminant-derived species, although definitive structural identification requires further analysis. The results of this study give new fundamental insight into the origin and migration of nitrogen-, nitrogen oxide-, and halogen-containing species in plastic waste pyrolysis oils. This knowledge can guide the design of more effective decontamination strategies and the development of novel additives and processing agents, which are essential for the large-scale implementation of chemical plastic waste recycling technologies.

## ■ ASSOCIATED CONTENT

### SI Supporting Information

The Supporting Information is available free of charge at <https://pubs.acs.org/doi/10.1021/acs.energyfuels.5c04213>.

The FT-ICR MS results of pure hydrocarbons; (+)-ESI FT-ICR MS results for N3O nitrogen oxides detected in waste PE and waste PP pyrolysis oil; complete set of (-)-ESI FT-ICR MS results for halogen-containing classes; and FT-ICR MS results of the detected <sup>13</sup>C-topologies (PDF)

## ■ AUTHOR INFORMATION

### Corresponding Author

Kevin M. Van Geem — *Laboratory for Chemical Technology, Department of Materials, Textiles and Chemical Engineering, Ghent University, 9052 Gent, Belgium; [orcid.org/0000-0003-4191-4960](https://orcid.org/0000-0003-4191-4960); Email: Kevin.VanGeem@UGent.be*

### Authors

Gilles Dossche — *Laboratory for Chemical Technology, Department of Materials, Textiles and Chemical Engineering, Ghent University, 9052 Gent, Belgium; [orcid.org/0001-5103-0208](https://orcid.org/0001-5103-0208)*

Yannick Ureel — *Laboratory for Chemical Technology, Department of Materials, Textiles and Chemical Engineering, Ghent University, 9052 Gent, Belgium; [orcid.org/0001-6883-320X](https://orcid.org/0001-6883-320X)*

Martha L. Aguilera — *Ion Cyclotron Resonance Program, National High Magnetic Field Laboratory, Florida State University, Tallahassee, Florida 32310, United States; International Joint Laboratory for Complex Matrices Molecular Characterization, iC2MC, TRTG, 76700 Harfleur, France; [orcid.org/0000-0002-7273-5343](https://orcid.org/0000-0002-7273-5343)*

Marvin Kusenberg — *Laboratory for Chemical Technology, Department of Materials, Textiles and Chemical Engineering, Ghent University, 9052 Gent, Belgium; [orcid.org/0000-0002-3733-3293](https://orcid.org/0000-0002-3733-3293)*

Ryan P. Rodgers — *Ion Cyclotron Resonance Program, National High Magnetic Field Laboratory, Florida State University, Tallahassee, Florida 32310, United States; International Joint Laboratory for Complex Matrices Molecular Characterization, iC2MC, TRTG, 76700 Harfleur, France; Department of Chemistry and Biochemistry, Florida State University, Tallahassee, Florida 32308, United States; [orcid.org/0000-0003-1302-2850](https://orcid.org/0000-0003-1302-2850)*

Maarten K. Sabbe — *Laboratory for Chemical Technology, Department of Materials, Textiles and Chemical Engineering, Ghent University, 9052 Gent, Belgium; [orcid.org/0000-0003-4824-2407](https://orcid.org/0000-0003-4824-2407)*

Complete contact information is available at: <https://pubs.acs.org/10.1021/acs.energyfuels.5c04213>

### Notes

The authors declare no competing financial interest.

## ■ ACKNOWLEDGMENTS

G.D. acknowledges the Fund for Scientific Research Flanders (FWO) for financial support via doctoral fellowship grant (1151825N). Y.U. acknowledges financial support from the FWO through the doctoral fellowship grant (1185822N). M.K. acknowledges financial support from the FWO through the postdoctoral fellowship grant (12ANG24N). A portion of this work was performed at the National High Magnetic Field Laboratory, which is supported by the National Science Foundation Division of Materials Research and Division of Chemistry through DMR-2128556 and the State of Florida. The authors acknowledge financial support by the catalistICON project(HBC.2018.0262) MATTER (Mechanical and Thermochemical Recycling of mixed plastic waste) funded by Flanders Innovation & Entrepreneurship (VLAIO).

## ■ ABBREVIATIONS

ABS,acrylonitrile butadiene styrene polymer; AIBN,azobisisobutyronitrile; CIC,combustion ion chromatography; CSTR,continuously stirred tank reactor; DBE,double bond equivalent; ESI,electrospray ionization; FID,flame ionization detector; FT-ICR MS,Fourier transform ion cyclotron resonance mass spectrometry; GC,gas chromatography; GC × GC,two-dimensional gas chromatography; ICP-OES,inductively coupled plasma optical emission spectroscopy; LDPE,low-density polyethylene; MPO,mixed polyolefins; MS,mass spectrometer; Mt,million tonnes; NCD,nitrogen chemiluminescence detector; PA,polyamides; PC,polycarbonate; PE,polyethylene; PET,polyethylene terephthalate; PIONA,paraffins, (iso-) paraffins, olefins, naphthalenes, aromatics; PP,polypropylene; PS,polystyrene; PUR,polyurethanes; PVC,polyvinyl chloride; PVDC,polyvinylidene chloride; RMS,root-mean-square

## ■ REFERENCES

- (1) Baekeland, L. H. The Synthesis, Constitution, and Uses of Bakelite. *Journal of Industrial & Engineering Chemistry* **1909**, *1* (3), 149–161.
- (2) OECD. *Global Plastics Outlook: Economic Drivers, Environmental Impacts and Policy Options*; OECD: Paris, 2022.
- (3) Van Geem, K. M. Plastic waste recycling is gaining momentum. *Science* **2023**, *381* (6658), 607–608.
- (4) Garcia, J. M.; Robertson, M. L. The future of plastics recycling. *Science* **2017**, *358* (6365), 870–872.
- (5) Ragaert, K.; Delva, L.; Van Geem, K. Mechanical and chemical recycling of solid plastic waste. *Waste Manag* **2017**, *69*, 24–58.
- (6) Schade, A.; Melzer, M.; Zimmermann, S.; Schwarz, T.; Stoewe, K.; Kuhn, H. Plastic Waste Recycling—A Chemical Recycling Perspective. *ACS Sustainable Chem. Eng.* **2024**, *12* (33), 12270–12288.
- (7) Achilias, D. S.; Giannoulis, A.; Papageorgiou, G. Z. Recycling of polymers from plastic packaging materials using the dissolution–reciprocation technique. *Polym. Bull.* **2009**, *63* (3), 449–465.

(8) Vollmer, I.; Jenks, M. J. F.; Roelands, M. C. P.; White, R. J.; van Harmelen, T.; de Wild, P.; et al. Beyond Mechanical Recycling: Giving New Life to Plastic Waste. *Angew. Chem., Int. Ed. Engl.* **2020**, *59* (36), 15402–15423.

(9) Jiang, J.; Shi, K.; Zhang, X.; Yu, K.; Zhang, H.; He, J.; et al. From plastic waste to wealth using chemical recycling: A review. *J. Environ. Chem. Eng.* **2022**, *10* (1), No. 106867.

(10) Chang, S. H. Plastic waste as pyrolysis feedstock for plastic oil production: A review. *Sci. Total Environ.* **2023**, *877*, No. 162719.

(11) Maqsood, T.; Dai, J.; Zhang, Y.; Guang, M.; Li, B. Pyrolysis of plastic species: A review of resources and products. *J. Anal. Appl. Pyrolysis* **2021**, *159*, No. 105295.

(12) Qureshi, M. S.; Oasmaa, A.; Pihkola, H.; Deviatkin, I.; Tenhunen, A.; Mannila, J.; et al. Pyrolysis of plastic waste: Opportunities and challenges. *J. Anal. Appl. Pyrolysis* **2020**, *152*, No. 104804.

(13) Kusenberg, M.; Zayoud, A.; Roosen, M.; Thi, H. D.; Abbas-Abadi, M. S.; Eschenbacher, A.; et al. A comprehensive experimental investigation of plastic waste pyrolysis oil quality and its dependence on the plastic waste composition. *Fuel Process. Technol.* **2022**, *227*, No. 107090.

(14) Toraman, H. E.; Dijkmans, T.; Djokic, M. R.; Van Geem, K. M.; Marin, G. B. Detailed compositional characterization of plastic waste pyrolysis oil by comprehensive two-dimensional gas-chromatography coupled to multiple detectors. *J. Chromatogr A* **2014**, *1359*, 237–246.

(15) Kusenberg, M.; Eschenbacher, A.; Djokic, M. R.; Zayoud, A.; Ragaert, K.; De Meester, S.; Van Geem, K. M. Opportunities and challenges for the application of post-consumer plastic waste pyrolysis oils as steam cracker feedstocks: To decontaminate or not to decontaminate? *Waste Manag* **2022**, *138*, 83–115.

(16) Baena-Gonzalez, J.; Santamaría-Echart, A.; Aguirre, J. L.; Gonzalez, S. Chemical recycling of plastic waste: Bitumen, solvents, and polystyrene from pyrolysis oil. *Waste Manag* **2020**, *118*, 139–149.

(17) Alfke, G.; Irion, W. W.; Neuwirth, O. S. Oil Refining. *Ullmann's Encyclopedia of Industrial Chemistry*; Wiley-VCH Verlag GmbH & Co. KGaA, **2007**.

(18) Charlesworth, J. M. Monitoring the products and kinetics of oil shale pyrolysis using simultaneous nitrogen specific and flame ionization detection. *Fuel* **1986**, *65* (7), 979–986.

(19) Lange, J.-P. Managing Plastic Waste—Sorting, Recycling, Disposal, and Product Redesign. *ACS Sustainable Chem. Eng.* **2021**, *9* (47), 15722–15738.

(20) Wang, C. Q.; Wang, H.; Fu, J. G.; Liu, Y. N. Flotation separation of waste plastics for recycling—A review. *Waste Manag* **2015**, *41*, 28–38.

(21) Havaei, M.; Akin, O.; Locaspi, A.; John Varghese, R.; Minette, F.; Romers, E.; et al. Beyond the Landfill: A critical review of techniques for End-of-Life Polyvinyl chloride (PVC) valorization. *Waste Manag* **2025**, *193*, 105–134.

(22) Gundupalli, S. P.; Hait, S.; Thakur, A. A review on automated sorting of source-separated municipal solid waste for recycling. *Waste Manag* **2017**, *60*, 56–74.

(23) Yoon, B. S.; Kim, C.; Park, G.-J.; Jeon, S. G.; Ko, C. H. Upgrading waste plastic pyrolysis oil via hydrotreating over sulfur-treated Ni-Mo/Al<sub>2</sub>O<sub>3</sub> catalysts. *Fuel* **2024**, *369*, No. 131688.

(24) Kusenberg, M.; Roosen, M.; Doktor, A.; Casado, L.; Jamil Abdulrahman, A.; Parvizi, B.; et al. Contaminant removal from plastic waste pyrolysis oil via depth filtration and the impact on chemical recycling: A simple solution with significant impact. *Chem. Eng. J.* **2023**, *473*, No. 145259.

(25) Zeb, W.; Roosen, M.; Knockaert, P.; Janssens, S.; Withoeck, D.; Kusenberg, M.; et al. Purification and characterisation of post-consumer plastic pyrolysis oil fractionated by vacuum distillation. *J. Clean. Prod.* **2023**, *416*, No. 137881.

(26) Yang, X.; Sun, L.; Xiang, J.; Hu, S.; Su, S. Pyrolysis and dehalogenation of plastics from waste electrical and electronic equipment (WEEE): a review. *Waste Manag* **2013**, *33* (2), 462–473.

(27) Abbas-Abadi, M. S.; Zayoud, A.; Kusenberg, M.; Roosen, M.; Vermeire, F.; Yazdani, P.; et al. Thermochemical recycling of end-of-life and virgin HDPE: A pilot-scale study. *J. Anal. Appl. Pyrolysis* **2022**, *166*, No. 105614.

(28) Perez, B. A.; Krishna, J. V. J.; Toraman, H. E. Characterization of polyolefins-based pyrolysis oils: A comparison between one-dimensional gas chromatography and two-dimensional gas chromatography. *J. Chromatogr A* **2025**, *1739*, No. 465510.

(29) Auersvald, M.; Šimánek, M.; Lyko Vachková, E.; Kroufek, J.; Straka, P.; Barzallo, G.; Vozka, P. A comparative study of aromatic content in pyrolysis oils from waste plastics and tires: Assessing common refinery methods. *Fuel* **2024**, *369*, No. 131714.

(30) Djokic, M. R.; Muller, H.; Ristic, N. D.; Akhras, A. R.; Symoens, S. H.; Marin, G. B.; Van Geem, K. M. Combined characterization using HT-GC × GC-FID and FT-ICR MS: A pyrolysis fuel oil case study. *Fuel Process. Technol.* **2018**, *182*, 15–25.

(31) Mase, C.; Maillard, J. F.; Paupy, B.; Farenc, M.; Adam, C.; Hubert-Roux, M.; et al. Molecular Characterization of a Mixed Plastic Pyrolysis Oil from Municipal Wastes by Direct Infusion Fourier Transform Ion Cyclotron Resonance Mass Spectrometry. *Energy Fuels* **2021**, *35* (18), 14828–14837.

(32) Hassibi, N.; Quiring, Y.; Carré, V.; Aubriet, F.; Vernex-Loset, L.; Mauviel, G.; Burké-Vitzthum, V. Analysis and control of products obtained from pyrolysis of polypropylene using a reflux semi-batch reactor and GC-MS/FID and FT-ICR MS. *J. Anal. Appl. Pyrolysis* **2023**, *169*, No. 105826.

(33) Ware, R. L.; Rowland, S. M.; Rodgers, R. P.; Marshall, A. G. Advanced Chemical Characterization of Pyrolysis Oils from Landfill Waste, Recycled Plastics, and Forestry Residue. *Energy Fuels* **2017**, *31* (8), 8210–8216.

(34) Ware, R. L.; Rowland, S. M.; Lu, J.; Rodgers, R. P.; Marshall, A. G. Compositional and Structural Analysis of Silica Gel Fractions from Municipal Waste Pyrolysis Oils. *Energy Fuels* **2018**, *32* (7), 7752–7761.

(35) Mase, C.; Maillard, J. F.; Paupy, B.; Hubert-Roux, M.; Afonso, C.; Giusti, P. Speciation and Semiquantification of Nitrogen-Containing Species in Complex Mixtures: Application to Plastic Pyrolysis Oil. *ACS Omega* **2022**, *7* (23), 19428–19436.

(36) Mase, C.; Maillard, J. F.; Piparo, M.; Friederici, L.; Ruger, C. P.; Marceau, S.; et al. GC-FTICR mass spectrometry with dopant assisted atmospheric pressure photoionization: application to the characterization of plastic pyrolysis oil. *Analyst* **2023**, *148* (20), 5221–5232.

(37) Dhahak, A.; Carre, V.; Aubriet, F.; Mauviel, G.; Burké-Vitzthum, V. Analysis of Products Obtained from Slow Pyrolysis of Poly(ethylene terephthalate) by Fourier Transform Ion Cyclotron Resonance Mass Spectrometry Coupled to Electrospray Ionization (ESI) and Laser Desorption Ionization (LDI). *Ind. Eng. Chem. Res.* **2020**, *59* (4), 1495–1504.

(38) Ureel, Y.; Chacón-Patiño, M. L.; Kusenberg, M.; Rodgers, R. P.; Sabbe, M. K.; Van Geem, K. M. Characterization of PP and PE Waste Pyrolysis Oils by Ultrahigh-Resolution Fourier Transform Ion Cyclotron Resonance Mass Spectrometry. *Energy Fuels* **2024**, *38* (12), 11148–11160.

(39) Ureel, Y.; Chacón-Patiño, M. L.; Kusenberg, M.; Ginzburg, A.; Rodgers, R. P.; Sabbe, M. K.; Van Geem, K. M. Compositional Analysis of Oxygenates and Hydrocarbons in Waste and Virgin Polyolefin Pyrolysis Oils by Ultrahigh-Resolution Fourier Transform Ion Cyclotron Resonance Mass Spectrometry. *Energy Fuels* **2025**, *39* (2), 1283–1295.

(40) Mase, C.; Sueur, M.; Lavanant, H.; Ruger, C. P.; Giusti, P.; Afonso, C. Ion Source Complementarity for Characterization of Complex Organic Mixtures Using Fourier Transform Mass Spectrometry: A Review. *Mass Spectrom. Rev.* **2024**, *44*, 808–829.

(41) Abbas-Abadi, M. S.; Kusenberg, M.; Zayoud, A.; Roosen, M.; Vermeire, F.; Madanikashani, S.; et al. Thermal pyrolysis of waste versus virgin polyolefin feedstocks: The role of pressure, temperature and waste composition. *Waste Manag* **2023**, *165*, 108–118.

(42) Smith, D. F.; Podgorski, D. C.; Rodgers, R. P.; Blakney, G. T.; Hendrickson, C. L. 21 T FT-ICR Mass Spectrometer for Ultrahigh-

Resolution Analysis of Complex Organic Mixtures. *Anal. Chem.* **2018**, *90* (3), 2041–2047.

(43) Cho, Y.; Ahmed, A.; Islam, A.; Kim, S. Developments in FT-ICR MS instrumentation, ionization techniques, and data interpretation methods for petroleomics. *Mass Spectrom Rev.* **2015**, *34* (2), 248–263.

(44) Chacón-Patiño, M. L.; Moulian, R.; Barrère-Mangote, C.; Putman, J. C.; Weisbrod, C. R.; Blakney, G. T.; et al. Compositional Trends for Total Vanadium Content and Vanadyl Porphyrins in Gel Permeation Chromatography Fractions Reveal Correlations between Asphaltene Aggregation and Ion Production Efficiency in Atmospheric Pressure Photoionization. *Energy Fuels* **2020**, *34* (12), 16158–16172.

(45) Weisbrod, C. R.; McKenna, A. M.; Hendrickson, C. L. Selective Gas-Phase Depletion of Chemical Contaminants in Dissolved Organic Matter Increases Compositional Coverage by FT-ICR Mass Spectrometry. *J. Am. Soc. Mass Spectrom.* **2024**, *35* (10), 2465–2471.

(46) Ugduler, S.; Van Geem, K. M.; Roosen, M.; Delbeke, E. I. P.; De Meester, S. Challenges and opportunities of solvent-based additive extraction methods for plastic recycling. *Waste Manag.* **2020**, *104*, 148–182.

(47) Weiss, I. M.; Muth, C.; Drumm, R.; Kirchner, H. O. K. Thermal decomposition of the amino acids glycine, cysteine, aspartic acid, asparagine, glutamic acid, glutamine, arginine and histidine. *BMC Biophys.* **2018**, *11*, 2.

(48) Oenema, J.; Liu, H.; Coensel, N. D.; Eschenbacher, A.; Van de Vijver, R.; Weng, J.; et al. Review on the pyrolysis products and thermal decomposition mechanisms of polyurethanes. *J. Anal. Appl. Pyrolysis* **2022**, *168*, No. 105723.

(49) Herrera, M.; Matuschek, G.; Kettrup, A. Main products and kinetics of the thermal degradation of polyamides. *Chemosphere* **2001**, *42* (5–7), 601–607.

(50) Chen, G.; Liu, T.; Luan, P.; Li, N.; Sun, Y.; Tao, J.; et al. Distribution, migration, and removal of N-containing products during polyurethane pyrolysis: A review. *J. Hazard Mater.* **2023**, *453*, No. 131406.

(51) Zhang, C.; Cui, F.; Zeng, G. M.; Jiang, M.; Yang, Z. Z.; Yu, Z. G.; et al. Quaternary ammonium compounds (QACs): a review on occurrence, fate and toxicity in the environment. *Sci. Total Environ.* **2015**, *518–519*, 352–362.

(52) Pappijn, C. A. R.; Vin, N.; Vermeire, F. H.; Van de Vijver, R.; Herbinet, O.; Battin-Leclerc, F.; et al. Experimental and kinetic modeling study of the pyrolysis and oxidation of diethylamine. *Fuel* **2020**, *275*, No. 117744.

(53) Perez, B. A.; Jayarama Krishna, J. V.; Toraman, H. E. Insights into co-pyrolysis of polyethylene terephthalate and polyamide 6 mixture through experiments, kinetic modeling and machine learning. *Chem. Eng. J.* **2023**, *468*, No. 143637.

(54) Zhang, H.; Jiang, X.; Wu, W.; Mo, Y. Electron conjugation versus pi-pi repulsion in substituted benzenes: why the carbon-nitrogen bond in nitrobenzene is longer than in aniline. *Phys. Chem. Chem. Phys.* **2016**, *18* (17), 11821–11828.

(55) Pappijn, C. A. R.; Vermeire, F. H.; Van de Vijver, R.; Reyniers, M.-F.; Marin, G. B.; Van Geem, K. M. Combustion of ethylamine, dimethylamine and diethylamine: Theoretical and kinetic modeling study. *Proceedings of the Combustion Institute* **2021**, *38* (1), 585–592.

(56) Collin, G.; Höke, H. Quinoline and Isoquinoline. *Ullmann's Encyclopedia of Industrial Chemistry*; Wiley-VCH Verlag GmbH & Co. KGaA, 2000.

(57) Pappijn, C. A. R.; Vermeire, F. H.; Van de Vijver, R.; Reyniers, M. F.; Marin, G. B.; Van Geem, K. M. Bond additivity corrections for CBS-QB3 calculated standard enthalpies of formation of H, C, O, N, and S containing species. *International Journal of Chemical Kinetics* **2021**, *53* (3), 345–355.

(58) Kim, Y. D.; Lee, J. J. An Investigation on Thermal Decomposition Behavior of Water-Soluble Azo Dyes. *Fibers Polym.* **2023**, *24* (8), 2799–2806.

(59) Nguyen, T. L.; Saleh, M. A. Thermal degradation of azobenzene dyes. *Results Chem.* **2020**, *2*, No. 100085.

(60) Rani, M.; Shim, W. J.; Han, G. M.; Jang, M.; Song, Y. K.; Hong, S. H. Benzotriazole-type ultraviolet stabilizers and antioxidants in plastic marine debris and their new products. *Sci. Total Environ.* **2017**, *579*, 745–754.

(61) Marchais, J.; Begue, D.; Dargelos, A.; Wentrup, C. Benzotriazoles and Triazoloquinones: Rearrangements to Carbazoles, Benzazirines, Azepinediones, and Fulvenimines. *J. Org. Chem.* **2021**, *86* (23), 16992–17001.

(62) Barker, S. J.; Storr, R. C. Flash-pyrolysis of 1-vinylbenzotriazoles. *J. Chem. Soc., Perkin Trans. 1* **1990**, *3*, 485–488.

(63) Tolinski, M. Processing Aids for Extrusion. *Additives for Polyolefins*; William Andrew Publishing, 2015; 135–144.

(64) Tolinski, M. Processing Aids for Molding. *Additives for Polyolefins*; William Andrew Publishing, 2015; 129–134.

(65) Jug, U.; Naumoska, K.; Metlicar, V.; Schink, A.; Makuc, D.; Vovk, I.; et al. Interference of oleamide with analytical and bioassay results. *Sci. Rep.* **2020**, *10* (1), 2163.

(66) Farajzadeh, M. A.; Ebrahimi, M.; Ranji, A.; Feyz, E.; Bejani, V.; Matin, A. A. HPLC and GC Methods for Determination of Lubricants and Their Evaluation in Analysis of Real Samples of Polyethylene. *Microchimica Acta* **2006**, *153* (1–2), 73–78.

(67) Lestido-Cardama, A.; Barbosa-Pereira, L.; Sendon, R.; Paseiro Losada, P.; de Quiros, A. R. B. Migration of Dihydroxy Alkylamines and Their Possible Impurities from Packaging into Foods and Food Simulants: Analysis and Safety Evaluation. *Polymers (Basel)* **2023**, *15* (12), 2656.

(68) Kellepan, V. T.; King, J. P.; Butler, C. S. G.; Williams, A. P.; Tuck, K. L.; Tabor, R. F. Heads or tails? The synthesis, self-assembly, properties and uses of betaine and betaine-like surfactants. *Adv. Colloid Interface Sci.* **2021**, *297*, No. 102528.

(69) Zhong, H.; Shi, Z.; Jiang, G.; Yuan, Z. Synergistic inhibitory effects of free nitrous acid and imidazoline derivative on metal corrosion in a simulated water injection system. *Water Res.* **2020**, *184*, No. 116122.

(70) Bajpai, D.; Tyagi, V. K. Fatty Imidazolines: Chemistry, Synthesis, Properties and Their Industrial Applications. *Journal of Oleo Science* **2006**, *55* (7), 319–329.

(71) Kirk-Othmer Encyclopedia of Chemical Technology; John Wiley & Sons, Inc.; 2000.

(72) Hansen, H. S.; Diep, T. A. N-acylethanolamines, anandamide and food intake. *Biochem. Pharmacol.* **2009**, *78* (6), 553–560.

(73) Harayama, T.; Riezman, H. Understanding the diversity of membrane lipid composition. *Nat. Rev. Mol. Cell Biol.* **2018**, *19* (5), 281–296.

(74) Zayoud, A.; Dao Thi, H.; Kusenberg, M.; Eschenbacher, A.; Kresovic, U.; Alderweireldt, N.; et al. Pyrolysis of end-of-life polystyrene in a pilot-scale reactor: Maximizing styrene production. *Waste Manag.* **2022**, *139*, 85–95.

(75) Çit, İ.; Sınak, A.; Yumak, T.; Uçar, S.; Misirlioğlu, Z.; Canel, M. Comparative pyrolysis of polyolefins (PP and LDPE) and PET. *Polym. Bull.* **2010**, *64* (8), 817–834.

(76) Prado, G. H. C.; Rao, Y.; de Klerk, A. Nitrogen Removal from Oil: A Review. *Energy Fuels* **2017**, *31* (1), 14–36.

(77) Kusenberg, M.; Eschenbacher, A.; Delva, L.; De Meester, S.; Delikontstantis, E.; Stefanidis, G. D.; et al. Towards high-quality petrochemical feedstocks from mixed plastic packaging waste via advanced recycling: The past, present and future. *Fuel Process. Technol.* **2022**, *238*, No. 107474.

(78) Marturano, V.; Cerruti, P.; Ambrogi, V. Polymer additives. *Phys. Sci. Rev.* **2017**, *2* (6), 20160130.

(79) Tamizhdurai, P.; Mangesh, V. L.; Santhosh, S.; Vedavalli, R.; Kavitha, C.; Bhutto, J. K.; et al. A state-of-the-art review of multilayer packaging recycling: Challenges, alternatives, and outlook. *J. Clean. Prod.* **2024**, *447*, No. 141403.

(80) Elias, H. G.; Mühlaupt, R. Plastics, General Survey, 2. Production of Polymers and Plastics. *Ullmann's Encyclopedia of Industrial Chemistry*; Wiley-VCH Verlag GmbH & Co. KGaA, 2015; 1–38.

(81) Heldt, H.-W.; Piechulla, B. Lipids are membrane constituents and function as carbon stores. *Plant Biochemistry*; Academic Press, 2011; 359–398.

(82) Blanco, A.; Blanco, G. Lipids. *Medical Biochemistry*; Academic Press, 2017; 99–119.

(83) Lau, O. W.; Wong, S. K. Contamination in food from packaging material. *J. Chromatogr A* **2000**, *882* (1–2), 255–270.

(84) Rollinson, A. *Leaky loop "recycling" - A technical correction on the quality of pyrolysis oil made from plastic waste*. In: Veillard, L.; Flynn, S., eds.; Zero Waste Europe, 2023.

(85) Baca, D.; Monroy, R.; Castillo, M.; Elkazraji, A.; Farooq, A.; Ahmad, R. Dioxins and plastic waste: A scientometric analysis and systematic literature review of the detection methods. *Environ. Adv.* **2023**, *13*, No. 100439.

(86) Paladino, O.; Moranda, A. Human Health Risk Assessment of a pilot-plant for catalytic pyrolysis of mixed waste plastics for fuel production. *J. Hazard Mater.* **2021**, *405*, No. 124222.



CAS BIOFINDER DISCOVERY PLATFORM™

## BRIDGE BIOLOGY AND CHEMISTRY FOR FASTER ANSWERS

Analyze target relationships,  
compound effects, and disease  
pathways

Explore the platform

